Hindawi Publishing Corporation
ISRN Materials Science
Volume 2013, Article ID 107178, 17 pages
http://dx.doi.org/10.1155/2013/107178

Review Article

Diffuse Scattering from Lead-Containing Ferroelectric Perovskite Oxides

D. J. Goossens

Research School of Chemistry, Australian National University, Canberra ACT 0200, Australia

Correspondence should be addressed to D. J. Goossens; goossens@rsc.anu.edu.au

Received 17 April 2013; Accepted 22 May 2013

Academic Editors: S. J. Milne and A. O. Neto

Ferroelectric materials rely on some type of non-centrosymmetric displacement correlations to give rise to a macroscopic polarisation. These displacements can show short-range order (SRO) that is reflective of the local chemistry, and so studying it reveals important information about how the structure gives rise to the technologically useful properties. A key means of exploring this SRO is diffuse scattering. Conventional structural studies use Bragg peak intensitiesto determine the average structure. In a single crystal diffuse scattering (SCDS) experiment, the coherent scattered intensity is measured at non-integer Miller indices, and can be used to examine the population of local configurations. This is because the diffuse scattering is sensitive to two-body averages, whereas the Bragg intensity gives single-body averages. This review outlines key results of SCDS studies on several materials and explores the similarities and differences in their diffuse scattering. Random strains are considered, as are models based on a phonon-like picture or a more local-chemistry oriented picture. Limitations of the technique are discussed.

1. Introduction

Single crystal diffuse scattering (SCDS) has been the subject of study since the earliest days of crystallography [1] and is seen in many patterns collected using film (e.g., [2]), film being an early variant of "area detector" and therefore very good for surveying large regions of reciprocal space—far better than an electronic point counter. The different forms of disorder present in crystalline materials, and how they are manifested in diffraction patterns have been well explored, both in monographs and papers (these include [3–14]).

Diffuse scattering can be defined for the purposes of this paper as the coherently scattered intensity that is *not* localised on the reciprocal lattice. It is the result of the two-body correlations in a crystalline material (see e.g., [15, 16]). These correlations may exist between atoms, molecules, and, in the case of neutron diffraction, magnetic moments [17–20].

It has long been known that diffuse scattering, an example is shown in Figure 1, contains information about the correlations in atomic and molecular thermal motions [21] as well as static short-range order. Modelling diffuse scattering is not simple, because locally the short-range order, SRO, need not obey the space group symmetry of the crystal. The global symmetry must be regained on averaging across the crystal but may not be present on the local scale of a few nanometres, or if one prefers, on the scale of a few unit cells. This renders many of the tools of conventional crystallography of limited use.

In particular, the idea of a single, repeating unit cell is not an adequate "solution" of the local structure—indeed, the very idea of what is meant by "structure solution" is thrown into question. Conventional crystallography solves (a better word may be "determines") very important aspects of the structure—those describing its global average. Analysis of SCDS reveals another important aspect—the pair correlations, and thus some deeper information on the population of local environments, which will be closely related to the crystal chemistry. But even SCDS is limited to two-body correlations. An experiment that could measure the phase shift of the scattered radiation (X-ray or neutron, in most cases) would be sensitive to higher-order correlations, and so on. At what level of detail one could consider the structure to be "solved" is almost a philosophical question. In practice, the level of detail depends on what is needed to give insight into the properties of the material. The structure is "solved" when the questions being asked can be answered.

Though not the subject of this review, it can be noted that diffuse scattering data collection is difficult.

The weak diffuse scattering must be measured in the presence of strong Bragg reflections, and so the experiments require low noise, high dynamic range, and detectors with good resistance to saturation [32, 33]. Data may require considerable correction and reconstruction [34–37] before they reach a useful format. Dedicated instruments for diffuse scattering are relatively rare, for example DNS at Jülich [20], D7 at the Institut Laue Langevin [19], Corelli at the Spallation Neutron Source [38], a custom-made laboratory X-ray machine [39, 40], the E2 flat cone instrument at the Helmholtz-Zentrum Berlin für Materialien und Energie [41], and so on. However, many other instruments are capable of collecting high quality data, including the powder diffractometer at the Australian Synchrotron [42], SXD at the ISIS neutron source [27, 43–45], Wombat at the OPAL reactor [35, 46], the SNBL beamline at ESRF [47], 11-ID-B at the Advanced Photon Source [48, 49], and others [50–52].

The correlation structure is likely to be anisotropic, such that a detailed model of the SRO will often require a three-dimensional (3D) dataset [23, 53–56], in turn implying the need to measure the distribution of weak and delocalised features throughout significant volumes of reciprocal space. This requires long experiments, very carefully characterised instruments, and large crystals—especially for neutron diffuse scattering. Even at a synchrotron a 3D dataset will take hours to collect, inhibiting studies as functions of temperature, pressure, and so on. If the crucial section of reciprocal space can be observed with a single crystal setting, such studies are practicable. This is perhaps made easier by using high X-ray energies that flatten the Ewald sphere such that a single exposure is almost flat in reciprocal space and can be made through sample orientation to coincide with some important symmetry directions. Hence a particular reciprocal space plane can, as long as it contains the origin, be captured in a single exposure if the crystal is appropriately aligned (Figure 1) [57, 58].

The importance of diffuse scattering in examining structures in ferroelectrics has long been recognised [59, 60], and highly structured diffuse scattering has been observed in many ferroelectric materials, including those of commercial importance: KDP (KH_2PO_4) [61], TGS ($(NH_2CH_2COOH)_3H_2SO_4$) [62], benzil ($C_{14}H_{10}O_2$) [2, 43, 63, 64], $BaTiO_3$ [59, 65], NBT ($Na_{0.5}Bi_{0.5}TiO_3$) [66], and so on.

Ferroelectric phenomena are inherently related to correlations amongst structural features, resulting as they do from electric dipoles due to ionic displacements [67]. As noted, it is well established that the diffraction images of $BaTiO_3$, a much-studied ferroelectric material, contain diffuse scattering (DS) [59, 65]. The observation of the evolution of the diffuse patterns through the ferroelectric phase transition [68] leads to ongoing debate over the character of the phase transition—for example, order-disorder as against displacive—in this material [69]. DS planes were observed and considered to be the result of displacements correlated in chains, with the correlations being either static or dynamic.

In the modern relaxor ferroelectric materials [70], DS has often been interpreted using the idea of domain-like

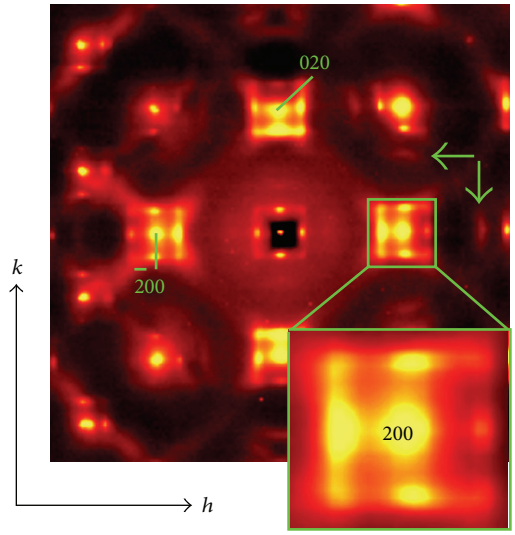

Figure 1: A single exposure from a stationary single crystal of wüstite, $Fe_{1-x}O$ (false colour map, white = high intensity). High-energy X-rays (65.35 keV in this case) give a small wavelength, λ, and an almost flat Ewald sphere. Hence these data closely approximate the $hk0$ section. Every Bragg reflection (and also the origin) is surrounded by a motif of incommensurate scattering. Second-order incommensurate spots have been arrowed and some Miller indices noted for scale [22].

polar nanoregions (PNRs) embedded in a paraelectric matrix, which are then linked to the outstanding electromechanical properties [71]. While the PNRs offer a convenient and somewhat intuitive model for the behaviour, the actual need for the concept is, according to some recent work, not thoroughly established [72]. It is also subtly different from the idea of ferroelectric nanodomains (FND) essentially "butting up" against each other—the main difference being the latter requires no paraelectric matrix.

Many of the most significant ferroelectric materials rely on lead, Pb, as a key ingredient in their crystal chemistry: PZT ($PbZr_{1-x}Ti_xO_3$) ([73–76] and others), PZN ($PbZn_{1/3}Nb_{2/3}O_3$) and PZN-PT ($PbZn_{1/3}Nb_{2/3}O_3$-$PbTiO_3$) ([76–78] and so on), and PMN ($PbMg_{1/3}Nb_{2/3}O_3$) and PMN-PT ($PbMg_{1/3}Nb_{2/3}O_3$-$PbTiO_3$) ([78–81] and others). The search for replacement Pb-free materials has often proceeded by analogy, with the obvious replacement for Pb^{2+} being Bi^{3+} ([82, 83] and many many more) and some exploration of Sn^{2+} [84–86], despite its difficult chemistry.

There are commonalities in the SCDS observed in many of the lead-based relaxors, particularly in their cubic phase [30, 87, 88]. A range of microscopic models have been developed to explain the systematics of the distribution of DS. Often these explanations draw on the idea of the PNR, whose geometry relates to the observed diffuse—atomic displacements correlated in two-dimensional sheets when the diffuse scattering is rod-like, one dimensional chains when the DS is sheet-like, and so on [27, 31, 44, 89–92].

A recent report by Bosak et al. [23] indicates that the diffuse scattering from these compounds can be modelled in a thermal-like way; in particular the often-referred-to diffuse

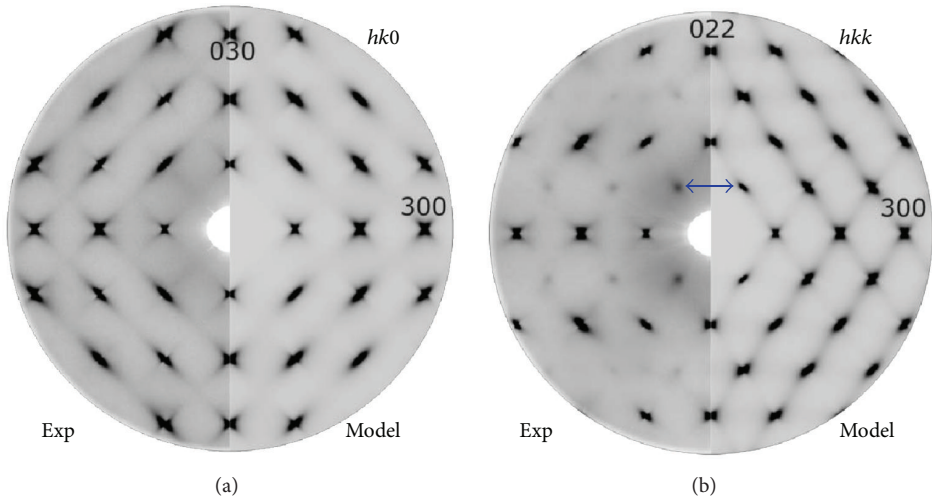

Figure 2: The quality of agreement between experimental data "exp" and calculation "model" is excellent in (a), perhaps less so in (b). (From Figure 4 of [23], used by permission of the IUCr, http://dx.doi.org/10.1107/S0108767311040281.)

"butterfly" (see the motif around the 300 peak in Figure 2) can be modelled using a purely thermal diffuse scattering-like approach that does not imply the existence of PNRs and has more in common with a phonon-based approach. This model uses parameters which are analogous to elastic constants, but are not elastic constants as such. It could be argued that of the two reciprocal space slices modelled in Figure 4 of [23] (reproduced in Figure 2) the second (*hkk*) is less than convincing; it seems to give streaks that are rather too strong and motifs of diffuse scattering which are too strong in every second horizontal row of features along the vertical axis (an example is arrowed by the current author on Figure 2(b)). Having said that, the model is clearly very powerful with very few parameters and shows that a displacement-wave picture rather than an order/disorder picture has much to recommend it. How the *B*-site randomness folds in to this is an interesting question, and it would be interesting to apply this approach to, for example, the PZT materials modelled in [25], in which the Pb-Pb ferroelectric domains were found to be of very different shape, being one-dimensional chains, and in which the static strains due to chemical disorder and *B*-site cation size mismatch are weaker and should therefore make a thermal-like model more applicable.

2. Survey of Diffuse Scattering in Pb-Based Ferroelectrics

2.1. $PbZr_{1-x}Ti_xO_3$. PZT, $PbZr_{1-x}Ti_xO_3$, ceramics are of great commercial importance and find uses as ultrasonic transducers in medical imaging, in accelerometers, and elsewhere [77, 93–96]. The structural phase diagram is summed up in Figure 3. The physical properties are optimal close to the morphotropic phase boundary, MPB, where the structure is prone to critical fluctuations and therefore responds more strongly to, for example, an external poling field. On the figure are noted (T, x) coordinates of the measurements discussed below.

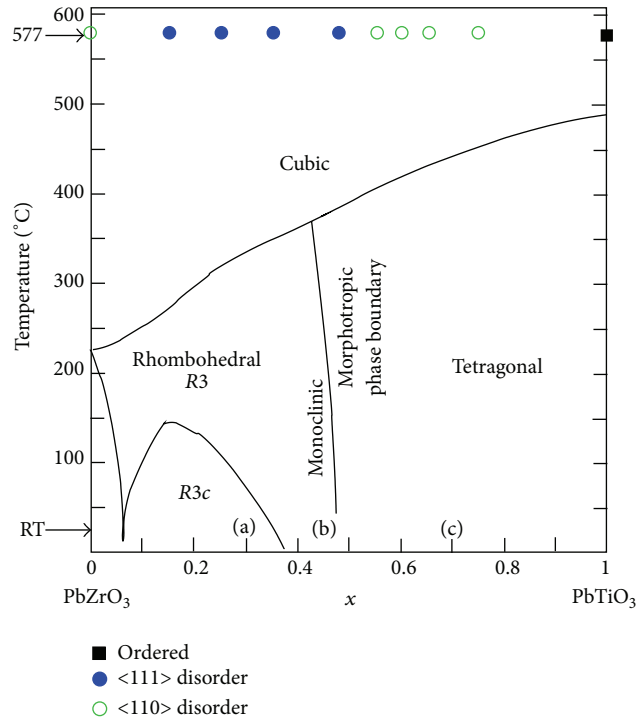

Figure 3: Schematic phase diagram for PZT. The morphotropic phase boundary is noted, along with key structural phases. Temperatures and x values for the various datasets discussed are noted on the figure—results at 577°C (850 K) are taken from [24], while letters (a), (b), and (c) correspond to diffraction patterns shown in Figure 4.

PT, $PbTiO_3$, appears to be a well-ordered perovskite [24, 97] with little diffuse scattering related to the PNR structures discussed here. Antiferroelectric PZ, $PbZrO_3$, on the other hand, does show diffuse scattering. The average structure at high temperatures shows $\langle 110 \rangle_p$ Pb^{2+} displacements [24]. Antiferroelectrically correlated displacements along one of

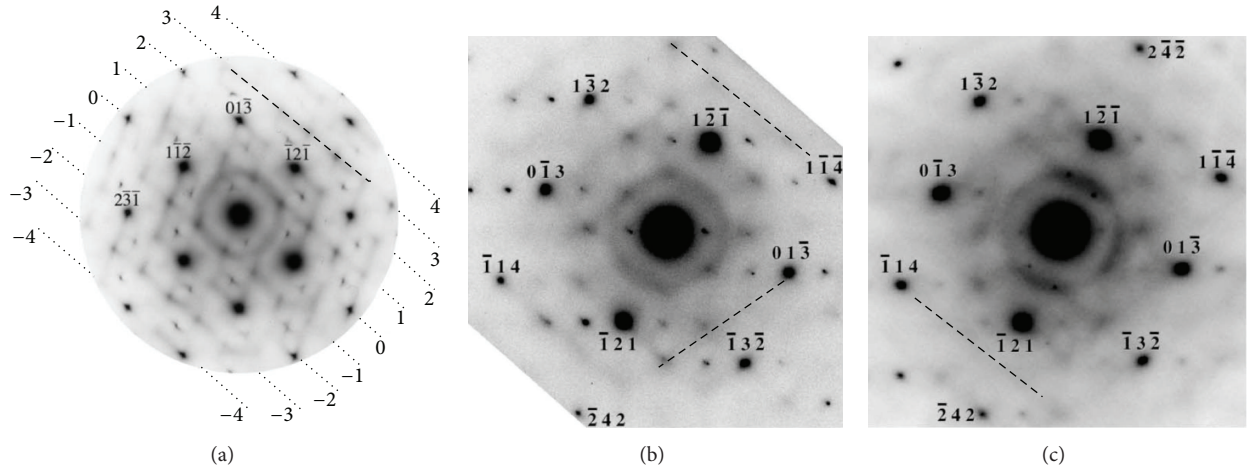

(a) (b) (c)

FIGURE 4: Observed electron diffuse scattering from PZT. (a) $PbZr_{1-x}Ti_xO_3$ with $x = 0.3$ (rhombohedral phase) viewed down the $[531]_c$ zone axis (c means relative to the cubic parent structure). (b) $x = 0.46$ (monoclinic) viewed down $[731]_c$. (c) $x = 0.7$ (tetragonal) viewed down $[731]_c$. Some reflections and lines of scattering have been marked.

the $[110]_p$ directions had been suggested in early diffraction work [98], though ordered—but with unrealistic degrees of octahedral distortion. This was largely remedied in terms of the average structure by introducing two substructures related by a shear of $c/2$ and allowing some disorder [99].

PDF work has since suggested that the Pb^{2+} are displaced at all temperatures, and the correlations amongst these displacements determine the observed average structure [100], including development of correlated c-axis displacements (compared to the antiferroelectric displacements in the bc plane) as expected to be associated with the weak room temperature piezoelectric effect in PZ [101]. Given the lack of B-site randomness, PNRs are unlikely to form if random strain fields (see below) play a role, and this is observed in PZ.

The average structure of PZT has been the subject of numerous studies (just a few include [24, 102–105]), and the work continues. It has been shown that at room temperature powder diffraction data are best modelled by a multiple-phase approach, in which the sample consists of a rhombohedral $R3c$ component and a monoclinic Cm component, with the proportion of Cm phase increasing with x (Ti content) as the MPB is approached [102]. Whether this is definitive or is an indication of the limits of powder diffraction in studying disordered materials is almost a question of ideology. It does appear that at high temperatures, in the cubic phase, the Pb atoms show disorder [24] that is not present in the Rietveld modelling [102], despite tests that were undertaken. Further, the presence of highly structured diffuse scattering in PZT at room temperature [25, 106–108] unambiguously *requires* an average crystal structure that permits local ordering to occur. Given that the Rietveld fits in [102] are of extremely high quality and yet do not yield models that permit SRO in Pb displacements to occur, it must be concluded that the powder diffraction is simply not sensitive to crucial aspects of the structure of PZT, despite the excellent fit statistics and the all-but perfect visual quality of the fits. This is a salutary lesson.

In the high-temperature cubic phase, it has been noted that the Pb atoms *do* show disorder. For $x = 0$ ($PbZrO_3$) they are distributed across 12 $\langle 110\rangle_c$-type directions (c implies indexing on the parent cubic structure); as Ti is doped in this, it switches to the 8 $\langle 111\rangle_c$-type directions, and until for $x > 0.5$ it switches back to the $\langle 110\rangle_c$-type directions, until at $x = 1$ ($PbTiO_3$) the Pb shows a single-ordered site [24]. Such a model accords extremely well with the modelling of electron diffuse scattering, which appears to show that the observed diffuse scattering can be explained by one-dimensional chains of Pb displacements that result in planes of diffuse scattering perpendicular to $\langle 111\rangle_c$ directions [107], and also accords well with neutron diffraction results [109]. Such a model was implemented using Monte Carlo simulation and was indeed found to reproduce many details of the observed electron diffuse scattering [25, 106]. As for other Pb^{2+} -based materials, the chronic underbonding of Pb^{2+} in the environment determined by the B-site cations (whose bonding is in a sense stiffer than the Pb-O bonds [110, 111]) is central to the mechanism of the off-centring.

Figure 5 shows a calculated diffraction pattern corresponding to in Figure 4(a), alongside a representation of the domain structure from the MC model. In this model, the Pb^{2+} are displaced along the eight $\langle 111\rangle_c$ shifts, but not in equal proportions. For the domain structure shown in Figure 5(a), ~51% of the Pb^{2+} are displaced along $[111]_c$, and this can be seen in the preponderance of red arrows (pointing up and to the right) in the figure. This imbalance is posited to drive the system away from cubic, and it may be conjectured that the average structure observed at high temperatures [24] is showing a state in which thermal energy is both evening out the distribution of Pb^{2+} displacements across the eight $\langle 111\rangle_c$ shifts and overwhelming the correlations between displacements, giving a real space picture of the structural phase transition as one in which the types of individual Pb^{2+} displacements do *not* change—though the proportions along the $\langle 111\rangle_c$ directions do—but the correlations amongst them

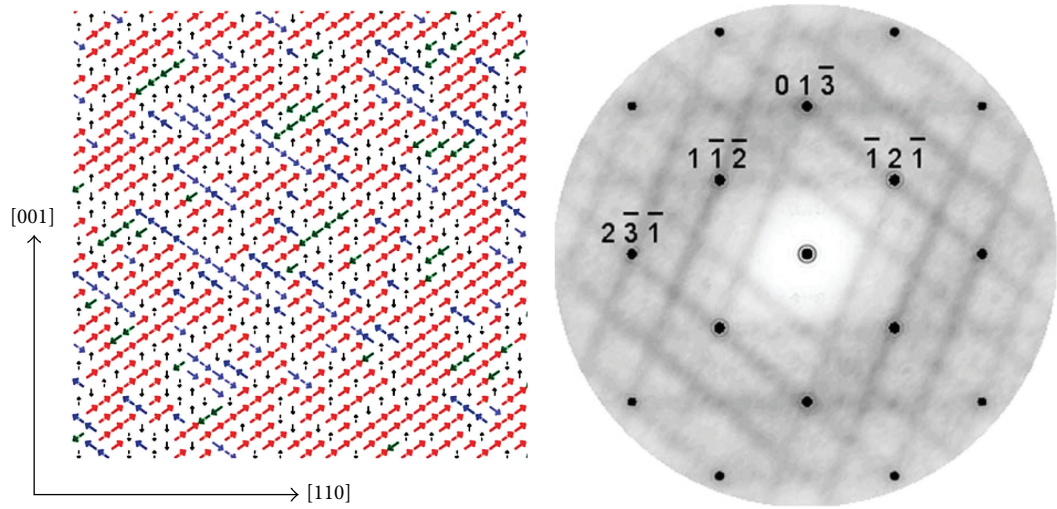

Figure 5: Calculated electron diffuse scattering from PZT. (a) The model domain structure and (b) the resulting diffraction pattern, to be compared to (a) in Figure 4 [25].

break down. Since the crystal chemistry around a given Pb^{2+} is not changing with T, this seems plausible.

Contrary to this atomistic model, a model in which inhomogeneous strains are caused by inclusions of a tetragonal phase within a rhombohedral or monoclinic matrix has been proposed [108]. On the basis of synchrotron diffuse and inelastic scattering the model reproduces some of the structure seen around selected Bragg peaks *via* these strain-inducing inclusions through a Huang-like formalism. This is qualitatively different from the relaxors like PMN-PT and PZN-PT, in which the Huang formalism cannot reproduce the observed scattering.

It is clear that the diffuse scattering in PZT varies strongly with composition [25, 106], as would be expected if random strain fields induced by *B*-site doping play a role in inhibiting long-range order in Pb^{2+} displacements and promoting nanodomain growth.

Interestingly, a Huang component has been observed in PMN above the Burns temperature, T_d [112], which is therefore not associated with domains but with "simple, isotropic defects" which are considered to be fluctuations in Nb^{5+} : Mg^{2+} concentrations on the nanoscale. This component of the diffuse scattering in PMN and related materials has been noted elsewhere [28, 113, 114]. It is relatively independent of temperature, being related to the chemical ordering on the *B*-site.

Earlier work using pair distribution function analysis showed that local structure in PZT and closely related La-doped PLZT ($[(Pb_{1-y}La_y)_{1-\alpha}\square_\alpha][(Zr_{1-x}Ti_x)_{1-\beta}\square_\beta]O_3$ or $(Pb_{1-3x/2}La_x)(Zr_yTi_{1-y})O_3$) was "more complex than that implied by the crystallographic structure" [115], with the PDF showing a wider range of Pb-O distances than the average structure suggests. The existence of short-range-ordered polar clusters has been suggested to explain Raman and other results in PLZT [116]. An electron diffraction study of $(Pb_{1-3x/2}La_x)(Zr_yTi_{1-y})O_3$ [117] draws related conclusions, noting that the "fundamental dipolar units in these materials correspond to highly anisotropic ⟨111⟩ chain dipoles formed from off-centre Pb/La and coupled Ti/Zr displacements."

Hence the overall picture is one in which the Pb^{2+} environments drive atomic Pb^{2+} displacements which interact *via* other atoms (in fact, *via* the BO_6 octahedra) and affect those other atoms. This is a common theme across the Pb^{2+} ferroic materials.

2.2. $PbZn_{1/3}Nb_{2/3}O_3$. Above T_C $PbZn_{1/3}Nb_{2/3}O_3$ (PZN) is cubic ($Pm\bar{3}m$) and average structure analysis that shows disordered off-centre displacements of Pb atoms [118]. According to early studies by Kuwata et al. [119, 120], on cooling PZN undergoes a phase transition to the rhombohedral phase [121, 122]. The existence of the R phase in bulk was questioned [91] after measurements of splitting of the (111) reflection, and an unusual bulk structure was posited in which a sample/grain showed a rhombohedral outer shell and a cubic inner core. This has been shown to be unnecessary [121, 122]. That PZN from $PbMg_{1/3}Nb_{2/3}O_3$ (PMN) which stays cubic down to 5 K [123]. It has been suggested that the phonon behaviour and diffuse scattering are very similar in the two materials [124].

You [125] recorded two-dimensional X-ray DS for PMN, showing "butterfly" and ellipsoidal-shaped DS, and related it to transverse optic soft modes producing correlations along the cubic ⟨110⟩ directions (later works have shown that a coupling of optic and acoustic-like displacements is needed to explain the intensity variation of DS in PMN [126]).

Some three-dimensional DS studies of PZN [27, 35, 44, 46] have applied $m\bar{3}m$ symmetry to the diffuse features even in the rhombohedral phase, as these appear to obey this symmetry within experimental resolution—the rhombohedral angle ~89.95°.

The diffuse scattering from PZN has been studied extensively. It was suggested that locally polarised "regions (probably of a size of the order of several unit cells)" could

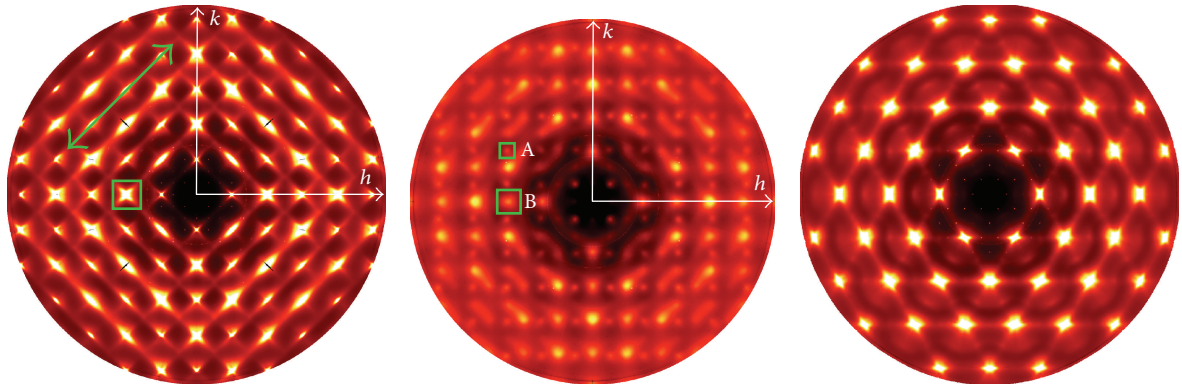

FIGURE 6: X-ray diffuse scattering from PZN, $PbZn_{1/3}Nb_{2/3}O_3$, showing the (a) $hk0$, (b) $hk0.5$, and (c) 111 sections of reciprocal space. Select features are highlighted. To indicate scale, note that the $\bar{2}00$ is boxed in (a) [26].

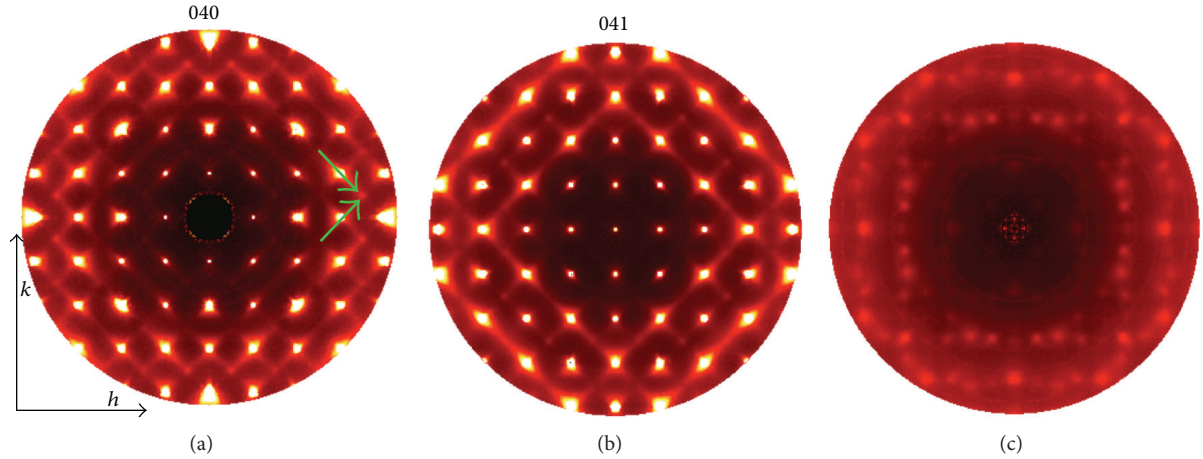

FIGURE 7: Neutron diffuse scattering from PZN, $PbZn_{1/3}Nb_{2/3}O_3$, showing the (a) $hk0$, (b) $hk1$, and (c) $hk0.5$ sections of reciprocal space. Select features are highlighted [27].

explain measurements of the index of refraction of PLZT ($(Pb_{1-3x/2}La_x)(Zr_yTi_{1-y})O_3$) and also the discovery of a second important temperature, the Burns temperature (T_d) well above T_C, above which it was posited that the domains ceased to exist [127]. PZN shows similar behaviour, with diffraction experiments showing that a signature for the posited domains could indeed be observed in the scattering from PZN and closely related PMN [126, 128, 129].

Using single high-energy X-ray exposures and tilting the sample, rather in the manner of a transmission electron microscope diffraction experiment, Xu and coworkers were able to show that the rods of scattering observed in PZN were indeed ⟨110⟩-type rods and not the intersections of, for example, the $hk0$ sections with out-of-plane rods in directions like ⟨111⟩ [54].

Figure 6 shows X-ray diffuse scattering in the $hk0$, $hk0.5$, and 111 sections of reciprocal space, measured on a single crystal of PZN at 300 K at the advanced photon source. These data clearly show the key diffuse features: the rods of scattering along ⟨110⟩-type directions (green arrow in Figure 6(a)), and the "butterfly" shapes where the rods intersect (boxed in Figure 6(a)), the ((1/2)(1/2)(1/2))-type spots that indicate *B*-site ordering (box "A" in Figure 6(b)) and that arise from intersection of the streaks with the layer (box "B" in Figure 6(b)). Also apparent is the variation of intensity along the length of the rods.

Figure 7 shows three slices of diffuse scattering, measured using neutron diffraction at the ISIS-pulsed neutron source. There is no energy analysis undertaken, and so the scattering is treated as wholly elastic. That this induces little or no loss of symmetry—as it does when the scattering is the result of phonons [43]—is indicative that the scattering is *not* of predominantly thermal origin, or that the thermal fluctuations are slow on the energy scale of thermal neutrons. Again, the key features are visible. More apparent than in Figure 6 is the size-effect scattering around, for example, the 004 Bragg peak and which is also apparent in the intensity of the ⟨110⟩ rods on the inside of a row of Bragg peaks compared to the outside (note green arrows showing direction of intensity transfer).

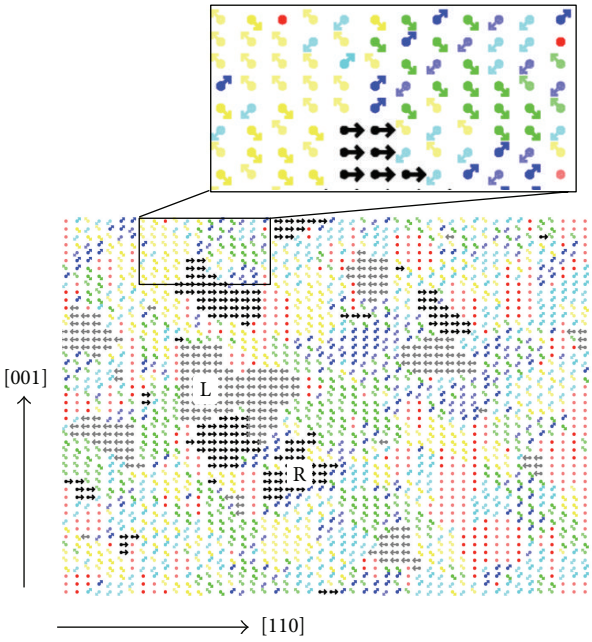

Figure 8: Schematic diagram of posited PNRs (domains) in PZN in the plane of one of the domains, axes as noted (section is normal to $[1\bar{1}0]$). Grey arrows lie in the plane and point left (L), black point right (R). Red (pink) dots point into (out of) the page. Other directions are intermediate.

The idea of a relatively static PNR lends itself to a local, atomistic model driven by the crystal chemistry—a real-space chemical picture rather than a reciprocal space phonon-based picture, as it was. Such a model is also reasonable given that local inhomogeneity appears to play a role in relaxor behaviour—relaxor behaviour is often induced by doping when the "pure" compound is a nonrelaxor ferroelectric. This is even the case in multiferroics, where the doping of $BiFeO_3$ with $BaTiO_3$ induces a change to relaxor-like behaviour [130, 131].

Hence, in modelling neutron diffuse scattering, Welberry and coworkers developed models for the diffuse scattering from PZN based on what could be termed chemical principles [27]. For example, the displacing of the Pb^{2+} ions is considered to be driven by the fact that Pb^{2+} is heavily underbonded in the average unit cell of PZN and also possesses an electron lone pair. The suggestion is that an inherently polar atom in a large environment (as parameterised by bond valence sums [132]) will satisfy its bonding requirements by moving off-centre rather than isotropically contracting its environment, and this is especially true of a "soft" atom like Pb^{2+} [133] which can be considered as sitting within a "hard" framework established by the oxygen atoms and the *B*-site cations.

The Pb atoms are considered to be displaced along ⟨110⟩-type directions in the unit cell, and these displacements are correlated within two-dimensional domains (see Figure 8), such that the displacement direction is parallel to a ⟨110⟩-type direction that lies within the plane of the domain. In essence, this is quite similar to the structure posted earlier based on diffuse X-ray scattering [54, 131]—except that there is no paraelectric matrix, but rather the volume is virtually entirely occupied by ferroelectric nanodomains (FND) of a range of sizes and orientations; this has led to the introduction of the term FND in distinction to PNR [72].

This model and its ramifications, including the response of the O ions to the Pb^{2+} framework and the alternating ordering of the Nb/Zn (frustrated by the 2 : 1 ratio of Nb to Zn), give rise to a qualitatively good agreement between observed and calculated data, including subtle details like the fact that every second diffuse rod is weak in the *hk*1 layer (Figure 7(b)). Further, the model gives an empirical chemical basis for the observed behaviour from which one can attempt to generalise in the search for Pb-free compounds. However, no underlying cause for the Pb^{2+} ions to form into the posited {110} domains is apparent.

More significantly, it has been shown that the simple heuristic interpretation of the diffuse scattering that leads to the displacement directions being of ⟨110⟩-type directions is misleading [89]. Investigation of these ideas shows that, at least in atomistic models, displacements indeed need not be along ⟨110⟩ directions, but that the domains themselves do need to be a single atomic layer thick, and with the established ⟨110⟩-type interfaces [134]. Having said that, high-temperature average structure determinations suggest that when the Pb site disorders, it is split across the 12 ⟨110⟩ directions [118]. Thus in some sense the initial model remains the best supported.

The question arises as to the power of the diffuse scattering to reveal the underlying structures. It has been shown that the diffuse scattering can be well modelled—and quantitatively—by a model that dispenses with static planar domains entirely [26]. This is supported by work discussed above [23] that also dispenses with PNRs and does a good job of modelling the scattering with just a handful of free parameters. Having said that, there is evidence that PNRs have been observed in relaxors using imaging techniques [135, 136] (with appropriate caveats about how representative of the bulk the surface may be), and so perhaps the ability to model the diffuse scattering with and without PNRs says more about the limits of the technique and the need to draw on multiple techniques than it says about PZN.

2.3. $PbMg_{1/3}Nb_{2/3}O_3$. Any discussion of $PbMg_{1/3}Nb_{2/3}O_3$-$PbTiO_3$ and $PbMg_{1/3}Nb_{2/3}O_3$ must relate to PZN, as the two materials are highly analogous.

$PbMg_{1/3}Nb_{2/3}O_3$ (PMN) is a heavily studied relaxor. Some work has used a dipole glass model to interpret diffuse scattering from PMN [137]. Earlier again it was suggested based on powder diffraction data that heavily displaced polar clusters of ions, particularly Pb^{2+} and O^{2-}, were required to model the average structure [123, 138]. Butterfly-shaped and ellipsoidal diffuse scattering was seen in X-ray diffraction experiments and explained in terms of transverse optic soft modes along the cubic ⟨110⟩ directions [125]. This has been elaborated more recently [126]. As with PZN, the polar nanoregion has been invoked, with the *T* dependence of the DS being attributed to the growth of PNRs with cooling [139].

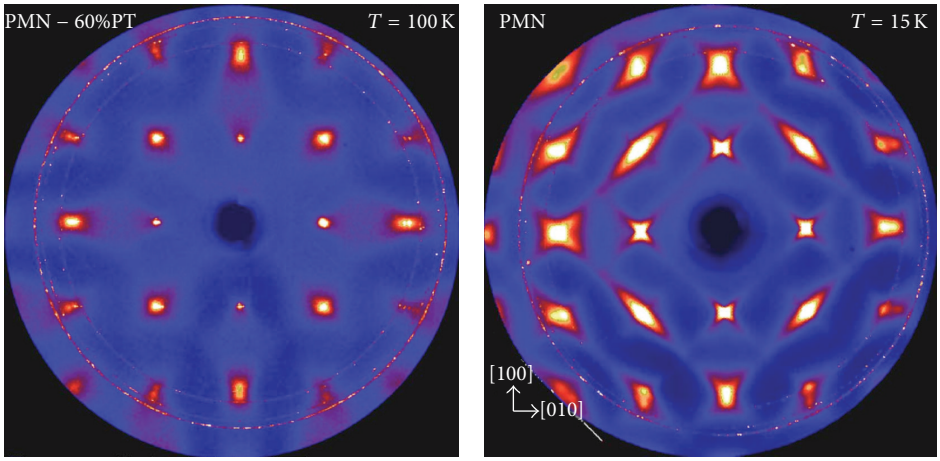

(a) (b)

FIGURE 9: Diffuse scattering in the *hk*0 layer of (a) PMN-60PT at 100 K and (b) PMN at 15 K. The radical change in the form of the scattering with PT fraction (x) and with T is apparent. Reprinted with permission from Figure 4 of [28] (http://link.aps.org/doi/10.1103/PhysRevB.73.064107). Copyright 2006 by the American Physical Society. (Readers may view, browse, and/or download material for temporary copying purposes only, provided that these uses are for noncommercial personal purposes. Except as provided by law, this material may not be further reproduced, distributed, transmitted, modified, adapted, performed, displayed, published, or sold in whole or part, without prior written permission from the American Physical Society.)

The relation of the lattice dynamics in PMN and PNRs (or local polar correlations) has been explored in some detail using a range of experimental techniques [140–144] and also ab initio calculations [145, 146].

As noted in the discussion of PZN, the diffuse scattering from $PbMg_{1/3}Nb_{2/3}O_3$-$PbTiO_3$ appears to be able to be parameterised using a thermal-like model that dispenses with PNRs [23, 147, 148] and also to be calculated from an ab initio approach [149] using recently established potentials [150]. Further molecular dynamics results suggest that Pb atoms show $\langle 111 \rangle_p$ displacements, as expected [151] and that while the PNR does seem to be a useful model for PMN at low temperatures [152], it is a sense-limiting case resulting from correlations that, while present at higher temperatures, do not necessarily produce domains as such. This is quite plausible; when there is substantial randomness in the system, *components* of the displacements can be correlated but a random component that increases with temperature may prevent them actually assembling into a physical domain in which all ions share a common displacement direction. Further, diffuse scattering is sensitive to pair correlations—without distinguishing between static and dynamic in the case of X-ray scattering of neutron energies well above the excitation energies—and so correlations amongst components of displacements on pairs of interacting atoms can show structure that is not apparent in the *absolute* displacements of the atoms. Importantly, these results depend on the local strains due to the *B*-site ordering of Nb and Mg as a mechanism for inhibiting large domains from forming, providing a strong link between *B*-site doping [153] and the introduction of relaxor behaviour [152]. An interesting comparison of scattering from PMN and PMN-60PT [28] shows that increasing PT doping greatly reduces the structure in the DS, leaving features that are weakly elongated in the radial direction (Figure 9). These have been interpreted as short-range chemical order scattering due to weak *B*-site ordering. As the *B*-site becomes heavily occupied by Ti^{4+}, the strains will grow weaker, removing the barrier to PNR growth and preventing the formation of the characteristic rods of $\langle 110 \rangle_p$ scattering.

Relatively straight-forward crystal chemical considerations and structural work [154, 155] show that the Pb^{2+} displacements are very large—typically 0.5 Å—which is why the treatment in [23] is "thermal-like" but not truly thermal. One approach to this has been to suggest that atomic shifts possess two components—one from a soft mode and the other a uniform displacement of the PNR [126].

On the assumption that the PNRs are real, diffuse scattering has been used to explore their response to applied field [156], and it is found that for a field applied along [001] the diffuse scattering in the (*hk*0) plane is affected, indicating a possible redistribution of nanodomains of different polarisations, at least those perpendicular to the field, as some become more energetically favourable than others. Similar effects have been modelled for PZN in the nanodomain picture [44] with good qualitative agreement with observations [92].

Further results, obtained by measuring diffuse scattering with different neutron energies to probe different time scales, suggest that the PNRs in PMN are (relatively) static [143] up to 420 K, and that the Burns temperature, as measured using diffuse scattering, may depend on the energy of the probe used—as the "static" PNRs become more dynamic above 420 K, they fluctuate on the timescale of a slow probe, but not a faster probe, causing different measurements of T_d and implying a switch from a slowly to more quickly fluctuating PNR state. This is similar to but different from molecular dynamics results which, when used to interpret

diffuse scattering over the range 10–700 K, suggest that strongly cooperative displacement behaviour sets in at 400 K on cooling [152]. This could also be interpreted as a value for T_d, as the PNRs/FNDs are the result of cooperative displacements.

Direct observation of PNRs through powder diffuse scattering (PDF analysis) has been claimed [151] though what actually manifests in the scattering are displacements and correlations. The work suggests that PNRs are "dispersed in a pseudocubic host lattice" [157] and that the PNRs begin to overlap as the sample cools to close to 200 K and increase in size and volume fraction of the sample but are affected by random fields due to the Mg/Nb disorder and are limited from growing further [158]. Other work also suggests 200 K as an important temperature—where possibly the domains truly manifest [152] and, most crucially, where the Curie temperature, T_C ~213 K [123, 138], is found. Hence, the overall picture is one in which on cooling correlations set in at T_d but do not necessarily induce an actual domain structure, at least not one in which the displacements do not possess a significant random component, with both correlated and uncorrelated components fluctuating in time and space; close to 200 K, the domains lock in, possibly as they start interacting with each other more strongly and stabilising their existence, and the Curie temperature is obtained.

2.4. $PbSc_{0.5}Nb_{0.5}O_3$ and $PbSc_{0.5}Ta_{0.5}O_3$. There are a range of other Pb-containing ferroic materials. Two significant materials are $PbSc_{0.5}Nb_{0.5}O_3$ and $PbSc_{0.5}Ta_{0.5}O_3$ [159, 160].

Diffuse scattering has been observed in $PbSc_{0.5}Ta_{0.5}O_3$ and derivatives [29, 161, 162] and is of similar form to that seen in PMN and PZN—rods of scattering perpendicular to ⟨110⟩ directions such that "the atomic ferroic shifts correlate within {110} planes of the real space" [29]. Studies as a function of pressure and Ba *A*-site doping "chemical pressure" suggest that pressure suppresses the diffuse scattering and decouples *B*-site/Pb displacements and is interpreted in terms of PNRs [161, 162]. The *B*-site stoichiometry of PST allows full anticorrelated ordering, which is seen in a cell doubling along all cubic directions. As a result, at room temperature, the diffuse scattering appears very similar to that from PZN; the diffuse spots which appear at (1/2)(1/2)(1/2)-type positions in PZN are sharp peaks occurring at 111-type positions for the doubled cell (Figure 10). That the increase in pressure suppresses the diffuse scattering accords with the bond valence picture of the driver for Pb^{2+} displacement, in that the Pb^{2+} environment will be reduced in size, lessening the need for displacement off-centre to increase the Pb^{2+}-bonding valence. This would also serve to decrease the *B*-site/Pb displacement correlations, as a Pb^{2+} which is "happier" in its bonding environment will distort the oxygen lattice to a smaller degree, reducing any transmitted effects.

At low *T*, the diffuse scattering becomes *less* pronounced because the polar order is quite long ranged. The intersection of the ⟨110⟩ diffuse streaks with the *hk*1 becomes more apparent though it can be discerned at 300 K.

Diffuse scattering has been observed in $PbSc_{0.5}Nb_{0.5}O_3$ as well [30, 163–165] and again tends to show the characteristic $\langle 110 \rangle_p$ (p = parent cell) diffuse streaks. These weaken substantially on cooling, rather like PST, whereas in doped PSN (with Ba and Bi in this very thorough study [30]) the diffuse scattering is more strongly maintained on cooling, something also apparent in Ba-doped PST [161]. This is strong evidence that, as discussed in relation to PMN, it is randomness that prevents the PNR from continuing to grow on cooling. In PST and PSN when the *B*-site cations are in a 1 : 1 ratio and can be strong ordered, such that there is a cell doubling, there is not the randomness that exists in PMN and PZN where the *B*-site cations are in ratio 2 : 1 and cannot alternate. Hence, on cooling, the PNR growth is less inhibited in PST/PSN, and the diffuse scattering sharpens to the point of almost vanishing—the ferroelectric order becomes virtually long ranged. This can be "remedied" by doping into the *A*-site, introducing greater disorder and restoring the randomness and preventing large domains from forming.

Average structure determination, allowing the Pb to disorder across split sites, has shown that the Pb^{2+} in PSN are indeed displaced (by ~0.40 Å at 2 K), but the displacement directions are not well determined by these neutron powder diffraction data [165]. The observed diffuse scattering in the powder diffraction background suggests that on cooling the "correlation among Pb displacements along $\langle 111 \rangle_{pc}$ directions increases to form polar domains" (pc = parent cell). They conclude that in the paraelectric phase the Pb^{2+} is distributed on many split sites around the Wyckoff position and that the minimum energy configuration changes with temperature, appearing to be most likely $\langle 111 \rangle_{pc}$ at lower temperatures and $\langle 100 \rangle_{pc}$ at the highest temperature considered.

2.5. $PbMg_{1/3}Ta_{2/3}O_3$. PMT, $PbMg_{1/3}Ta_{2/3}O_3$, is clearly related to PMN and PZN in terms of its chemistry, and it is perhaps not surprising that the diffuse scattering accords with this. PMT is a relaxor ferroelectric with a mean Curie temperature T_{cm} ~170 K [166].

Initial neutron diffuse scattering experiments used limited regions of reciprocal space—essentially, linear cuts through the (110) Bragg position [167]. These showed diffuse scattering whose intensity increased and width fell as *T* was reduced from room temperature to 100 K. These quantities then remained constant down to 20 K. The results suggested that displacements were static at low temperature and gave a low temperature correlation length, ξ, of $\xi \sim 39$ Å below 100 K, smaller than that has been suggested for PZN [137]. Given that the size difference between Mg and Ta is the largest exhibited in these Pb^{2+} containing compounds (the R_{ij} [132] for relevant species are: Mg^{2+} 1.693 Å, Zn^{2+}: 1.704 Å, Nb^{5+}: 1.911 Å, Ta^{5+}: 1.92 Å, and Sc^{3+}: 1.849 Å). Hence the *B*-site randomness coupled to the most pronounced size difference gives rise to the strongest random strain field and serves to inhibit large domain growth. In PSN and PST, where the *B*-site cations are present in a 1 : 1 ratio and a relatively more similar in size, the domains seem able to grow so large, as *T* is reduced that the diffuse scattering coalesces into sharp features (Figure 10).

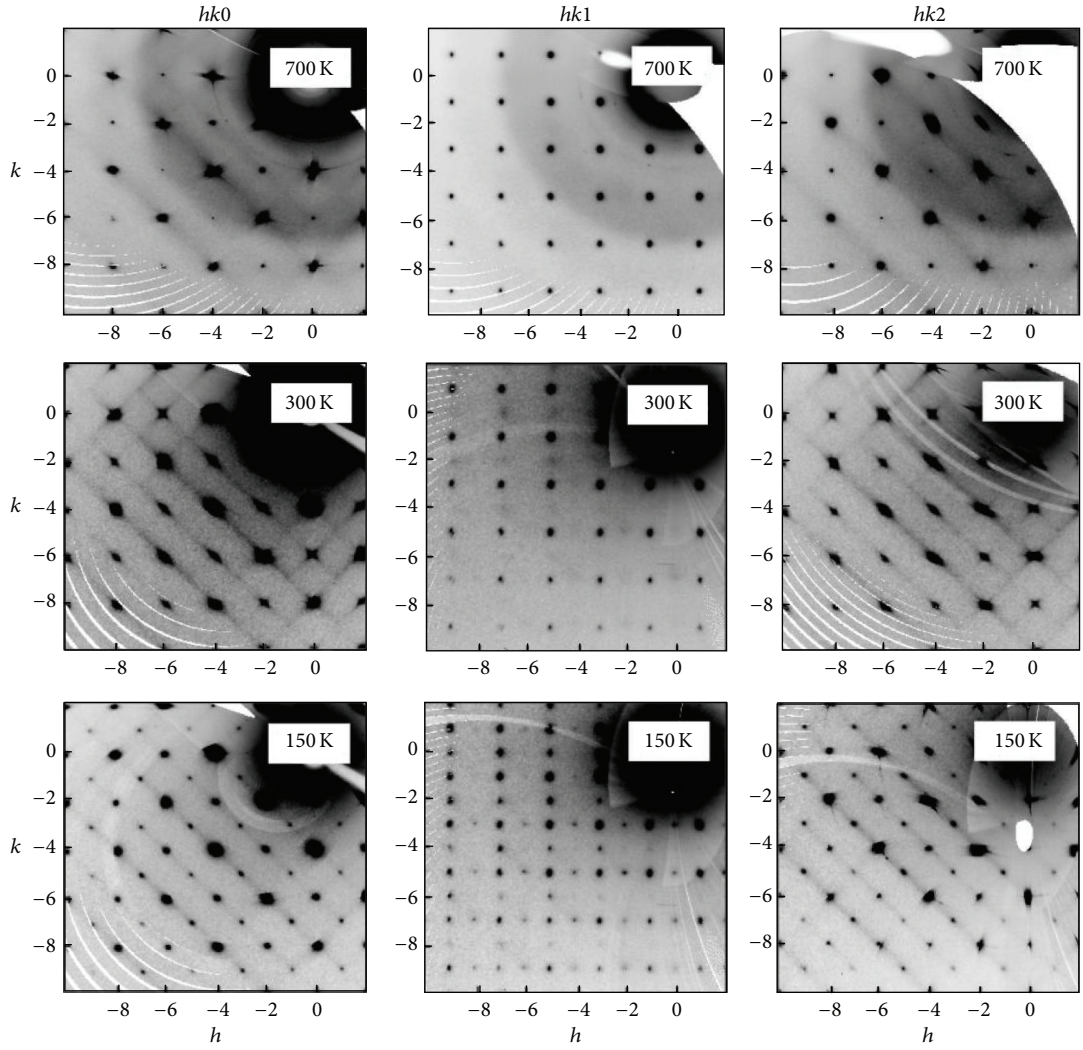

FIGURE 10: X-ray diffuse scattering from $PbSc_{0.5}Ta_{0.5}O_3$ as a function of temperature. The unit cell here is doubled relative to the parent perovskite cube. Note that the diffuse features at 300 K are very similar to those present in Figures 6 and 7, allowing that the indices here are doubled. Images taken with permission from [29] (http://hasyweb.desy.de/science/annual_reports/2007_report/part1/contrib/42/20848.pdf) and Figure 1 of [30] (http://link.aps.org/doi/10.1103/PhysRevB.79.224108). Copyright 2009 by the American Physical Society (see the following: Readers may view, browse, and/or download material for temporary copying purposes only, provided that these uses are for noncommercial personal purposes. Except as provided by law, this material may not be further reproduced, distributed, transmitted, modified, adapted, performed, displayed, published, or sold in whole or part, without prior written permission from the American Physical Society).

Data collected over wider regions of reciprocal space using synchrotron X-rays at 175 K shows similar structure to that observed in PMN and PZN [31] (Figure 11) including evidence for partial *B*-site ordering.

These data are modelled with Pb^{2+} displacements along $\langle 111 \rangle_{pc}$ and anisotropic PNRs whose longest dimension is in $\langle 110 \rangle_{pc}$. PNR dimensions were estimated as $\sim 7a_{pc} \times 7a_{pc} \times 20a_{pc}$ (a_{pc} being parent perovskite cube dimension). This is not greatly larger than the other estimate [167], except for the long axis which is approximately doubled. It should be noted however that the agreement between Figures 2 and 3 in [31] is moderate. The model does not capture the $\langle 110 \rangle_{pc}$ rods of diffuse scattering that connect the motifs of scattering around the Bragg peaks. Figure 12 shows a line profile, integrated over a wide band of pixels, taken in the direction of the broad black outline arrow in Figure 11(a). It has been fitted with a Gaussian on a linear background and shows quite clearly that, though weak, the diffuse scattering extends right through the Brillouin zone and is not localised in the vicinity of the Bragg spots. This large extent in reciprocal space strongly suggests that the PNRs do indeed need to be more pancake-like in real space than the model presented in [31] suggests, only enhancing their similarity to those in PMN and PZN.

3. Conclusions

It appears that diffuse scattering, both single crystal and powder, does indeed give deep insight into the structure of these materials, but it does not deliver "unique" solutions but constrains the possible solutions. Into the future,

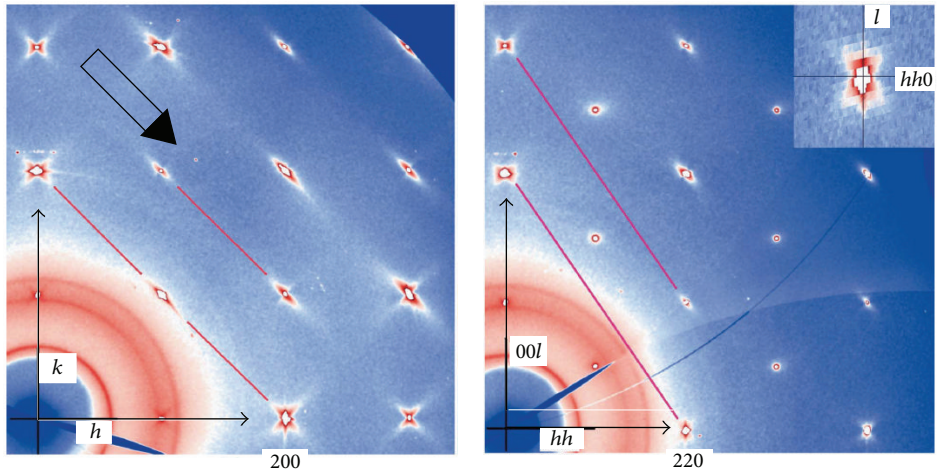

Figure 11: X-ray diffuse scattering from $PbMg_{1/3}Ta_{2/3}O_3$ in the (a) *hk*0 and (b) *hhl* planes, showing similar structure to that observed in PMN and PZN. The inset shows a close view of the 220 Bragg peak and the surrounding diffuse scattering. (Figure from [31], with permission of the IUCr, http://dx.doi.org/10.1107/S0021889811012635.)

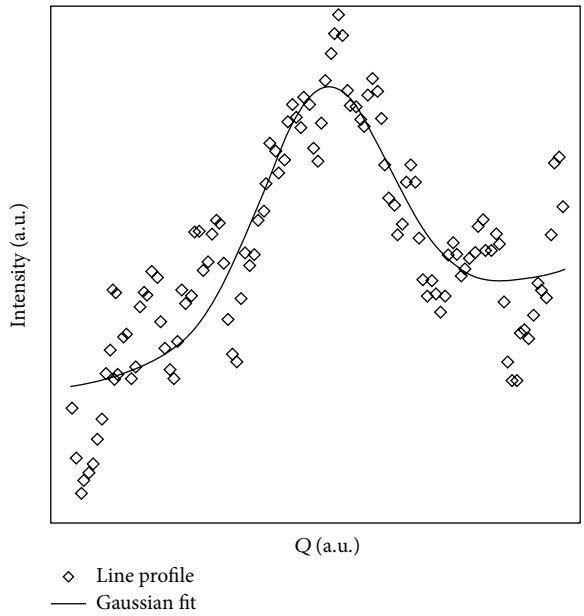

Figure 12: A line profile through the diffuse scattering shown in Figure 11(a), along the direction of the black arrow, demonstrating that the streaks of scattering do not just form "butterflies" and similar shapes around the Bragg spots, but also extend through reciprocal space much like those in PZN (Figure 6).

energy-analysed diffuse scattering is likely to play an important role, as it provides insights onto the dynamic or static nature of the local correlations, adding important new information to the picture. Further, it is clear that modelling large windows of reciprocal space and preferably three-dimensional volumes are important when the scattering is so anisotropic and extended. Some models work well close to Bragg positions but less well near reciprocal cell boundaries, showing that measuring comprehensive data is necessary if models are to be adequately tested.

The Pb-based relaxors show great commonality of behaviour and similarities in their diffuse scattering. It appears that the idea of the PNR (or FND) may not be mathematically necessary to describe the locus of the diffuse scattering but nevertheless has a strong basis in crystal chemistry, electron imaging, and molecular dynamics modelling and still appears to be a reasonable model for the local order. The questions of whether the domains are static or dynamic and what aspects of their behaviour are crucial in determining the properties are yet to be fully resolved across the family. Is a domain truly an observable polarised volume of the crystal, like a small (often one- or two-dimensional) ferroic crystal embedded in the larger, or is it a relatively evanescent region in which some components of the displacements are correlated while others are random? As yet no definitive picture has emerged although measurements on both PZN and PMN suggest that the PNRs are fluctuating relatively slowly on the time scale of a thermal neutron experiment, which is not to say that random components of the displacements are not fluctuating much faster. It does appear that randomness, whether *B*-site or *A*-site, plays a central role, with the size mismatch and the level of doping being, along with T relative to T_d, key in determining the degree of PNR-related scattering.

The overall picture is one in which the Pb^{2+} ion is too small to "sit" in the centre of the O environment determined by the stiffer *B*-site-to-oxygen bonds, and as an inherently polar atom due to its unpaired electrons resolves this by moving off-centre. In systems with chemical disorder, these shifts are prevented from becoming long-range ordered even at low T by the random strain fields caused to the size mismatch of the *B*-site cations (or *A*-site when applicable, as in Ba-doped PST). Hence the nature of the local order and that of the relaxor properties appear to be determined by both the average Pb^{2+} environment and by the distribution of local

environments—for example, PZ shows Pb^{2+} displacements but not PNRs, while PT, where Ti^{4+} is substantially smaller than Zr^{4+} [168], appears to show an ordered Pb^{2+} site, as might be more likely given that the *A*-site environment is smaller and so the Pb^{2+} is less underbonded; and PZN and its derivatives and close relatives, with significant randomness, do show the PNR scattering.

Acknowledgments

Thanks are due to the Australian Research Council for support through its Discovery Projects Program. D. J. Goossens thanks Dr. A. P. Heerdegen, Professor T. R. Welberry, Dr. Marek Pas'ciak, Dr. Jessica Hudspeth, and Ross Whitfield of the Research School of Chemistry at the Australian National University for their advice and assistance, but they take no responsibilities for any inaccuracies or opinions expressed herein. The support of the Australian Institute of Nuclear Science and Engineering is appreciated. Thanks are due to Professor Dr. Boriana Mihailova for supplying images used in Figure 10. Use of the Advanced Photon Source, an Office of Science User Facility operated for the U.S. Department of Energy (DOE) Office of Science by Argonne National Laboratory, was supported by the U.S. DOE under Contract no. DE-AC02-06CH11357. The granting of permission to reproduce figures from the noted publications is appreciated. Some aspects of this research were undertaken on the NCI National Facility in Canberra, Australia, which is supported by the Australian Commonwealth Government.

References

[1] W. Friedrich, "Röntgenstrahlinterferenzen," *Physikalische Zeitschrift*, vol. 14, pp. 1079–1087, 1913.

[2] K. Lonsdale and H. Smith, "An experimental study of diffuse x-ray reflexion by single crystals," *Proceedings of the Royal Society A*, vol. 179, pp. 8–50.

[3] R. I. Barabash, G. E. Ice, and P. E. A. Turchi, *Diffuse Scattering and the Fundamental Properties of Materials*, Momentum Press, 1st edition, 2009.

[4] M. A. Krivoglaz, *Diffuse Scattering of X-Rays and Neutrons by Fluctuations*, Springer, Berlin, Germany, 1996.

[5] M. A. Krivoglaz, *Theory of X-Ray and Thermal-Neutron Scattering by Real Crystals*, Plenum Press, New York, NY, USA, 1969.

[6] D. W. L. Hukins, *X-Ray Diffraction by Ordered and Disorderd Systems*, Pergamon Press, New York, NY, USA, 1981.

[7] W. A. Wooster, *Diffuse X-Ray Reflections from Crystals*, Clarendon Press, Oxford, UK, 1962.

[8] T. R. Welberry, *Diffuse X-Ray Scattering and Models of Disorder*, Oxford University Press, 2004.

[9] G. Harburn, C. A. Taylor, and T. R. Welberry, *Atlas of Optical Transforms*, Bell, London, UK, 1975.

[10] Th. Proffen, "Analysis of occupational and displacive disorder using the atomic pair distribution function: a systematic investigation," *Zeitschrift fur Kristallographie*, vol. 215, no. 11, pp. 661–668, 2000.

[11] W. Schweika, *Disordered Alloys: Diffuse Scattering and Monte Carlo Simulations*, Springer, 1998.

[12] R. B. Neder and Th. Proffen, *Diffuse Scattering and Defect Structure Simulations: A Cook Book Using the Program DISCUS*, OUP, 2008.

[13] V. M. Nield and D. A. Keen, *Diffuse Neutron Scattering from Crystalline Materials*, OUP, Oxford, UK, 2001.

[14] S. J. L. Billinge and M. F. Thorpe, *Local Structure from Diffraction*, Plenum, New York, NY, USA, 1998.

[15] B. D. Butler and T. R. Welberry, "Interpretation of displacement-caused diffuse scattering using the Taylor expansion," *Acta Crystallographica A*, vol. 49, no. 5, pp. 736–743, 1993.

[16] B. E. Warren, B. L. Averbach, and B. W. Roberts, "Atomic size effect in the x-ray scattering by alloys," *Journal of Applied Physics*, vol. 22, no. 12, pp. 1493–1496, 1951.

[17] T. J. Hicks, "Experiments with neutron polarization analysis," *Advances in Physics*, vol. 45, no. 4, pp. 243–298, 1996.

[18] T. J. Hicks, *Magnetism in Disorder*, OUP, 1995.

[19] J. R. Stewart, P. P. Deen, K. H. Andersen et al., "Disordered materials studied using neutron polarization analysis on the multi-detector spectrometer, D7," *Journal of Applied Crystallography*, vol. 42, no. 1, pp. 69–84, 2009.

[20] W. Schweika and P. Böni, "The instrument DNS: polarization analysis for diffuse neutron scattering," *Physica B*, vol. 297, pp. 155–159, 2001.

[21] H. Faxén, "Die bei interferenz von röntgenstrahlen infolge der wärmebewegung entstehende streustrahlung," *Zeitschrift für Physik*, vol. 17, pp. 266–278, 1923.

[22] T. R. Welberry and A. G. Christy, "Defect distribution and the diffuse x-ray diffraction pattern of wüstite, $Fe_{1-x}O$," *Physics and Chemistry of Minerals*, vol. 24, pp. 24–38, 1997.

[23] A. Bosak, D. Chernyshov, S. Vakhrushev, and M. Krisch, "Diffuse scattering in relaxor ferroelectrics: true three-dimensional mapping, experimental artefacts and modelling," *Acta Crystallographica A*, vol. 68, no. 1, pp. 117–123, 2012.

[24] Y. Kuroiwa, Y. Terado, S. J. Kim et al., "High-energy SR powder diffraction evidence of multisite disorder of Pb atom in cubic phase of $PbZr_{1-x}TixO_3$," *Japanese Journal of Applied Physics A*, vol. 44, no. 9B, pp. 7151–7155, 2005.

[25] T. R. Welberry, D. J. Goossens, R. L. Withers, and K. Z. Baba-Kishi, "Monte Carlo simulation study of diffuse scattering in PZT, Pb(Zr,Ti)O 3," *Metallurgical and Materials Transactions A*, vol. 41, no. 5, pp. 1110–1118, 2010.

[26] M. Paściak, A. P. Heerdegen, D. J. Goossens, R. E. Whitfield, A. Pietraszko, and T. R. Welberry, "Assessing local structure in $PbZn_{1/3}Nb_{2/3}O_3$ using diffuse scattering and reverse Monte Carlo refinement," *Metallurgical and Materials Transactions A*, vol. 44, pp. 87–93, 2013.

[27] T. R. Welberry, M. J. Gutmann, H. Woo et al., "Single-crystal neutron diffuse scattering and Monte Carlo study of the relaxor ferroelectric $PbZn_{1/3}Nb_{2/3}O_3$ (PZN)," *Journal of Applied Crystallography*, vol. 38, no. 4, pp. 639–647, 2005.

[28] C. Stock, D. Ellis, I. P. Swainson et al., "Damped soft phonons and diffuse scattering in 40%Pb $(Mg_{1/3}Nb_{2/3})O_3$-60%$PbTiO_3$," *Physical Review B*, vol. 73, no. 6, Article ID 064107, 2006.

[29] B. Mihailova, B. Maier, C. Paulmann et al., "High-temperature structural transformations in the relaxor ferroelectrics $PbSc_{0.5}Ta_{0.5}O_3$ and $Pb_{0.78}Ba_{0.22}Sc_{0.5}Ta_{0.5}O_3$," *Physical Review B*, vol. 77, no. 17, Article ID 174106, 2008.

[30] B. Maier, B. Mihailova, C. Paulmann et al., "Effect of local elastic strain on the structure of Pb-based relaxors: a comparative study of pure and Ba- and Bi-doped $PbSc_{0.5}Nb_{0.5}O_3$," *Physical Review B*, vol. 79, Article ID 224108, 2009.

[31] A. Cervellino, S. N. Gvasaliya, O. Zaharko et al., "Diffuse scattering from the lead-based relaxor ferroelectric $PbMg_{1/3}Ta_{2/3}O_3$," *Journal of Applied Crystallography*, vol. 44, no. 3, pp. 603–609, 2011.

[32] T. R. Welberry, D. J. Goossens, A. P. Heerdegen, and P. L. Lee, "Problems in measuring diffuse X-ray scattering," *Zeitschrift fur Kristallographie*, vol. 220, no. 12, pp. 1052–1058, 2005.

[33] H. Jagodzinski and F. Frey, *International Tables for Crystallography*, vol. B, 2006.

[34] M. J. Gutmann, *SXD2001*, ISIS Facility, Rutherford Appleton Laboratory, Oxfordshire, UK, 2005.

[35] R. E. Whitfield, D. J. Goossens, A. J. Studer, and J. S. Forrester, "Measuring single-crystal diffuse neutron scattering on the wombat high-intensity powder diffractometer," *Metallurgical and Materials Transactions A*, vol. 43, pp. 1423–1428, 2012.

[36] M. A. Estermann and W. Steurer, "Diffuse scattering data acquisition techniques," *Phase Transitions*, vol. 67, no. 1, pp. 165–195, 1998.

[37] S. Scheidegger, M. A. Estermann, and W. Steurer, "Correction of specimen absorption in X-ray diffuse scattering experiments with area-detector systems," *Journal of Applied Crystallography*, vol. 33, no. 1, pp. 35–48, 2000.

[38] S. Rosenkranz and R. Osborn, "Corelli: efficient single crystal diffraction with elastic discrimination," *Pramana*, vol. 71, no. 4, pp. 705–711, 2008.

[39] J. C. Osborn and T. R. Welberry, "A position-sensitive detector system for the measurement of diffuse X-ray scattering," *Journal of Applied Crystallography*, vol. 23, pp. 476–484, 1990.

[40] H. J. Lamfers, *A Diffuse X-Ray Scattering Diffractometer*, Rijksuniversiteit Groningen, 1997.

[41] R. Born and D. Hohlwein, "Simultaneous energy analysis in a large angular range: A novel neutron spectrometer, its resolution and applications," *Zeitschrift für Physik B Condensed Matter*, vol. 74, no. 4, pp. 547–555, 1989.

[42] E. J. Chan and D. J. Goossens, "Study of the single-crystal X-ray diffuse scattering in paracetamol polymorphs," *Acta Crystallographica B*, vol. 68, pp. 80–88, 2012.

[43] T. R. Welberry, D. J. Goossens, W. I. F. David, M. J. Gutmann, M. J. Bull, and A. P. Heerdegen, "Diffuse neutron scattering in benzil, C14D10O2, using the time-of-flight Laue technique," *Journal of Applied Crystallography*, vol. 36, no. 6, pp. 1440–1447, 2003.

[44] T. R. Welberry, D. J. Goossens, and M. J. Gutmann, "Chemical origin of nanoscale polar domains in PbZn1 3 Nb2 3 O_3," *Physical Review B*, vol. 74, no. 22, Article ID 224108, 2006.

[45] D. J. Goossens, A. G. Beasley, T. R. Welberry, M. J. Gutmann, and R. O. Piltz, "Neutron diffuse scattering in deuterated paraterphenyl, C 18D14," *Journal of Physics Condensed Matter*, vol. 21, no. 12, Article ID 124204, 2009.

[46] R. E. Whitfield, D. J. Goossens, and A. J. Studer, "Temperature dependence of diffuse scattering in PZN," *Metallurgical and Materials Transactions A*, vol. 43, pp. 1429–1433, 2012.

[47] A. Cervellino, S. N. Gvasaliya, B. Roessli et al., "Cube-shaped diffuse scattering and the ground state of $BaMg_{1/3}Ta_{2/3}O_3$," *Physical Review B*, vol. 86, Article ID 104107, 12 pages, 2012.

[48] E. J. Chan, T. R. Welberry, D. J. Goossens, and A. P. Heerdegen, "A refinement strategy for Monte Carlo modelling of diffuse scattering from molecular crystal systems," *Journal of Applied Crystallography*, vol. 43, no. 4, pp. 913–915, 2010.

[49] E. J. Chan, T. R. Welberry, D. J. Goossens, A. P. Heerdegen, A. G. Beasley, and P. J. Chupas, "Single-crystal diffuse scattering studies on polymorphs of molecular crystals. I. the room-temperature polymorphs of the drug benzocaine," *Acta Crystallographica B*, vol. 65, no. 3, pp. 382–392, 2009.

[50] N. Ahmed, S. J. Campbell, and T. J. Hicks, "LONGPOL II: analysis of spin-flip and nonspin-flip neutron scattering," *Journal of Physics E*, vol. 7, no. 3, article no. 318, pp. 199–204, 1974.

[51] T. Ersez, S. J. Kennedy, T. J. Hicks, Y. Fei, Th. Krist, and P. A. Miles, "New features of the long-wavelength polarisation analysis spectrometer—LONGPOL," *Physica B*, vol. 335, no. 1–4, pp. 183–187, 2003.

[52] E. Elkaim, S. Lefebvre, R. Kahn, J. F. Berar, M. Lemonnier, and M. Bessiere, "Diffraction and diffuse scattering measurements in material science: Improvement brought to a six-circle goniometer on a synchrotron beam line," *Review of Scientific Instruments*, vol. 63, no. 1, pp. 988–991, 1992.

[53] M. W. Wall, S. E. Ealick, and S. M. Gruner, "Three-dimensional diffuse x-ray scattering from crystals of *Staphylococcal* nuclease," *Proceedings of the National Academy of Sciences of the United States of America*, vol. 94, pp. 6180–6184, 1997.

[54] G. Xu, Z. Zhong, H. Hiraka, and G. Shirane, "Three-dimensional mapping of diffuse scattering in $Pb(Zn_{1/3}Nb_{2/3})O_{3-x}PbTiO_3$," *Physical Review B*, vol. 70, Article ID 174109, 17 pages, 2004.

[55] T. Weber and H.-B. Bürgi, "Determination and refinement of disordered crystal structures using evolutionary algorithms in combination with Monte Carlo methods," *Acta Crystallographica A*, vol. 58, pp. 526–540, 2002.

[56] T. Weber, A. Simon, H. Mattausch, L. Kienle, and O. Oeckler, "Reliability of Monte Carlo simulations of disordered structures optimized with evolutionary algorithms exemplified with diffuse scattering from $La_{0.70(1)}(Al_{0.14(1)}I_{0.86(1)})$," *Acta Crystallographica A*, vol. 64, no. 6, pp. 641–653, 2008.

[57] T. R. Welberry, D. J. Goossens, D. R. Haeffner, P. L. Lee, and J. Almer, "High-energy diffuse scattering on the 1-ID beamline at the advanced photon source," *Journal of Synchrotron Radiation*, vol. 10, no. 3, pp. 284–286, 2003.

[58] A. Gibaud, D. Harlow, J. B. Hastings, J. P. Hill, and D. Chapman, "A high-energy monochromatic laue (monolaue) X-ray diffuse scattering study of KMnF3 using an image plate," *Journal of Applied Crystallography*, vol. 30, no. 1, pp. 16–20, 1997.

[59] G. Honjo, S. Kodera, and N. Kitamura, "Diffuse streak diffraction patterns from single crystals I. General discussion and aspects of electron diffraction diffuse streak patterns," *Journal of the Physical Society of Japan*, vol. 19, no. 3, pp. 351–367, 1964.

[60] C. Randall, D. Barber, R. Whatmore, and P. Groves, "Short-range order phenomena in lead-based perovskites," *Ferroelectrics*, vol. 76, Article ID 1, pp. 277–282, 1987.

[61] S. R. Andrews and R. A. Cowley, "X-ray scattering from critical fluctuations and domain walls in KDP and DKDP," *Journal of Physics C*, vol. 19, no. 4, 1986.

[62] Y. Fujii and Y. Yamada, "X-ray critical scattering in ferroelectric tri-glycine sulphate," *Journal of the Physical Society of Japan*, vol. 30, no. 6, pp. 1676–1685, 1971.

[63] D. J. Goossens, A. P. Heerdegen, T. R. Welberry, and M. J. Gutmann, "Monte Carlo analysis of neutron diffuse scattering data," *Physica B*, vol. 385-386, pp. 1352–1354, 2006.

[64] T. R. Welberry, D. J. Goossens, A. J. Edwards, and W. I. F. David, "Diffuse X-ray scattering from benzil, C14H10O2: Analysis via automatic refinement of a Monte Carlo model," *Acta Crystallographica A*, vol. 57, no. 1, pp. 101–109, 2001.

[65] J. Harada and G. Honjo, "X-ray studies of the lattice vibration in tetragonal barium titanate," *Journal of the Physical Society of Japan*, vol. 22, no. 1, pp. 45–57, 1967.

[66] J. Kreisel, P. Bouvier, B. Dkhil et al., "Effect of high pressure on the relaxor ferroelectrics $Na_{1/2}Bi_{1/2}TiO_3$ (NBT) and $PbMg_{1/3}Nb_{2/3}O_3$ (PMN)," *Ferroelectrics*, vol. 302, pp. 293–298, 2004.

[67] J. F. Scott, "Prospects for ferroelectrics: 2012–2022," *ISRN Materials Science*, vol. 2013, Article ID 187313, 24 pages, 2013.

[68] R. Comes, M. Lambert, and A. Guinier, "The chain structure of $BaTiO_3$ and $KNbO_3$," *Solid State Communications*, vol. 6, no. 10, pp. 715–719, 1968.

[69] J. Hlinka, T. Ostapchuk, D. Nuzhnyy et al., "Coexistence of the phonon and relaxation soft modes in the terahertz dielectric response of tetragonal $BaTiO_3$," *Physical Review Letters*, vol. 101, no. 16, Article ID 167402, 2008.

[70] L. E. Cross, "Relaxor ferroelectrics," *Ferroelectrics*, vol. 76, pp. 241–267, 1987.

[71] A. A. Bokov and Z.-G. Ye, "Recent progress in relaxor ferroelectrics with perovskite structure," *Journal of Materials Science*, vol. 41, no. 1, pp. 31–52, 2006.

[72] J. Hlinka, "Do we need the ether of polar nanoregions?" *Journal of Advanced Dielectrics*, vol. 2, no. 2, Article ID 1241006, 2012.

[73] C. R. Martin and I. A. Aksay, "Topographical evolution of lead zirconate titanate (PZT) thin films patterned by micromolding in capillaries," *Journal of Physical Chemistry B*, vol. 107, no. 18, pp. 4261–4268, 2003.

[74] R. Bogue, "Energy harvesting and wireless sensors: a review of recent developments," *Sensor Review*, vol. 29, no. 3, pp. 194–199, 2009.

[75] N. Setter, D. Damjanovic, L. Eng et al., "Ferroelectric thin films: rsssssssseview of materials, properties, and applications," *Journal of Applied Physics*, vol. 100, no. 5, Article ID 051606, 2006.

[76] M. Sitti, D. Campolo, J. Yan et al., "Development of PZT and PZN-PT based unimorph actuators for micromechanical flapping mechanisms," in *Proceedings of the IEEE International Conference on Robotics and Automation (ICRA '01)*, vol. 4, pp. 3839–3846, May 2001.

[77] S. E. Park and W. Hackenberger, "High performance single crystal piezoelectrics: Applications and issues," *Current Opinion in Solid State and Materials Science*, vol. 6, no. 1, pp. 11–18, 2002.

[78] L. A. Ivan, M. Rakotondrabe, J. Agnus et al., "Comparative material study between PZT ceramic and newer crystalline PMN-PT and PZN-PT materials for composite bimorph actuators," *Reviews on Advanced Materials Science*, vol. 24, no. 1-2, pp. 1–9, 2010.

[79] H. Uršič, M. S. Zarnik, and M. Kosec, "$Pb(Mg_{1/3}Nb_{2/3})O_3$-$PbTiO_3$ (PMN-PT) material for actuator applications," *Smart Materials Research*, vol. 2011, Article ID 452901, 6 pages, 2011.

[80] S. H. Baek, J. Park, D. M. Kim et al., "Giant piezoelectricity on Si for hyperactive MEMS," *Science*, vol. 334, no. 6058, pp. 958–961, 2011.

[81] M. Frank, K. S. Moon, and S. Kassegne, "A PMMA coated PMN-PT single crystal resonator for sensing chemical agents," *Smart Materials and Structures*, vol. 19, no. 3, Article ID 035015, 2010.

[82] T. Takenaka, "Piezoelectric properties of some lead-free ferroelectric ceramics," *Ferroelectrics*, vol. 230, no. 1, pp. 87–98, 1999.

[83] E. A. Patterson and D. P. Cann, "Bipolar piezoelectric fatigue of $Bi(Zn_{0.5}Ti_{0.5})O_3$-$(Bi_{0.5}K_{0.5})TiO_3$-$(Bi_{0.5}Na_{0.5})TiO_3$ Pb-free ceramics," *Applied Physics Letters*, vol. 101, no. 4, Article ID 042905, 2012.

[84] J. W. Bennett, I. Grinberg, P. K. Davies, and A. M. Rappe, "Pb-free ferroelectrics investigated with density functional theory: $SnAl_{1/2}Nb_{1/2}O_3$ perovskites," *Physical Review B*, vol. 83, Article ID 144112, 6 pages, 2011.

[85] Y. Uratani, T. Shishidou, and T. Oguchi, "First-principles study of lead-free piezoelectric $SnTiO_3$," *Japanese Journal of Applied Physics*, vol. 47, no. 9, pp. 7735–7739, 2008.

[86] A. I. Lebedev, "Ab initio calculations of phonon spectra in $ATiO_3$ perovskite crystals (A = Ca, Sr, Ba, Ra, Cd, Zn, Mg, Ge, Sn, Pb)," *Physics of the Solid State*, vol. 51, no. 2, pp. 362–372, 2009.

[87] B. Mihailova, B. Maier, C. Paulmann et al., "High-temperature structural transformations in the relaxor ferroelectrics $PbSc_{0.5}Ta_{0.5}O_3$ and $Pb_{0.78}Ba_{0.22}Sc_{0.5}Ta_{0.5}O_3$," *Physical Review B*, vol. 77, Article ID 174106, 10 pages, 2008.

[88] P. Ganesh, E. Cockayne, M. Ahart et al., "Origin of diffuse scattering in relaxor ferroelectrics," *Physical Review B*, vol. 81, no. 14, Article ID 144102, 2010.

[89] M. Paściak, M. Wołcyrz, and A. Pietraszko, "Interpretation of the diffuse scattering in Pb-based relaxor ferroelectrics in terms of three-dimensional nanodomains of the ⟨110⟩-directed relative interdomain atomic shifts," *Physical Review B*, vol. 76, no. 1, Article ID 014117, 2007.

[90] T. R. Welberry and D. J. Goossens, "The interpretation and analysis of diffuse scattering using Monte Carlo simulation methods," *Acta Crystallographica A*, vol. 64, no. 1, pp. 23–32, 2007.

[91] G. Xu, Z. Zhong, Y. Bing, Z.-G. Ye, C. Stock, and G. Shirane, "Ground state of the relaxor ferroelectric $Pb(Zn_{1/3}Nb_{2/3})O_3$," *Physical Review B*, vol. 67, Article ID 104102, 5 pages, 2003.

[92] G. Xu, Z. Zhong, Y. Bing, Z.-G. Ye, and G. Shirane, "Electric-field-induced redistribution of polar nano-regions in a relaxor ferroelectric," *Nature Materials*, vol. 5, no. 2, pp. 134–140, 2006.

[93] T. R. Gururaja, R. K. Panda, J. Chen, and H. Beck, "Single crystal transducers for medical imaging applications," in *Proceedings of the IEEE Ultrasonics Symposium*, pp. 969–972, October 1999.

[94] Q. F. Zhou, H. L. W. Chan, and C. L. Choy, "PZT ceramic/ceramic 0–3 nanocomposite films for ultrasonic transducer applications," *Thin Solid Films*, vol. 375, no. 1-2, pp. 95–99, 2000.

[95] L. Lebrun, G. Sebald, B. Guiffard, C. Richard, D. Guyomar, and E. Pleska, "Investigations on ferroelectric PMN-PT and PZN-PT single crystals ability for power or resonant actuators," *Ultrasonics*, vol. 42, no. 1-9, pp. 501–505, 2004.

[96] Z. Yang, X. Chao, R. Zhang, Y. Chang, and Y. Chen, "Fabrication and electrical characteristics of piezoelectric PMN-PZN-PZT ceramic transformers," *Materials Science and Engineering B*, vol. 138, no. 3, pp. 277–283, 2007.

[97] B. D. Chapman, E. A. Stern, S.-W. Han et al., "Diffuse x-ray scattering in perovskite ferroelectrics," *Physical Review B*, vol. 71, no. 2, Article ID 020102, 2005.

[98] E. Sawaguchi, H. Maniwa, and S. Hoshino, "Antiferroelectric structure of lead zirconate," *Physical Review*, vol. 83, no. 5, p. 1078, 1951.

[99] A. M. Glazer, K. Roleder, and J. Dec, "Structure and disorder in single-crystal lead zirconate, $PbZrO_3$," *Acta Crystallographica B*, vol. 49, no. 5, pp. 846–852, 1993.

[100] S. Teslic and T. Egami, "Atomic structure of $PbZrO_3$ determined by pulsed neutron diffraction," *Acta Crystallographica B*, vol. 54, no. 6, pp. 750–765, 1998.

[101] X. Dai, J. Li, and D. Viehland, "Weak ferroelectricity in antiferroelectric lead zirconate," *Physical Review B*, vol. 51, no. 5, pp. 2651–2655, 1995.

[102] H. Yokota, N. Zhang, A. E. Taylor, P. A. Thomas, and A. M. Glazer, "Crystal structure of the rhombohedral phase of $PbZr_{1-x}TixO_3$ ceramics at room temperature," *Physical Review B*, vol. 80, Article ID 104109, 12 pages, 2009.

[103] J. Frantti, S. Ivanov, S. Eriksson et al., "Neutron diffraction and bond-valence calculation studies of $Pb(Zr_xTi_{1-x})O_3$ Ceramics," *Ferroelectrics*, vol. 272, no. 1, pp. 51–56, 2002.

[104] J. Ricote, D. L. Corker, R. W. Whatmore et al., "A TEM and neutron diffraction study of the local structure in the rhombohedral phase of lead zirconate titanate," *Journal of Physics Condensed Matter*, vol. 10, no. 8, pp. 1767–1786, 1998.

[105] D. Viehland, Z. Xu, and D. A. Payne, "Origin of F spots and stress sensitivity in lanthanum lead zirconate titanate," *Journal of Applied Physics*, vol. 74, no. 12, pp. 7454–7460, 1993.

[106] K. Z. Baba-Kishi, T. R. Welberry, and R. L. Withers, "An electron diffraction and Monte Carlo simulation study of diffuse scattering in $Pb(Zr,Ti)O_3$," *Journal of Applied Crystallography*, vol. 41, no. 5, pp. 930–938, 2008.

[107] A. M. Glazer, P. A. Thomas, K. Z. Baba-Kishi, G. K. H. Pang, and C. W. Tai, "Influence of short-range and long-range order on the evolution of the morphotropic phase boundary in $Pb(Zr_{1-x}Ti_x)O_3$," *Physical Review B*, vol. 70, Article ID 184123, 9 pages, 2004.

[108] R. G. Burkovsky, A. Yu. Bronwald, A. V. Filimonov et al., "Structural heterogeneity and diffuse scattering in morphotropic lead zirconate-titanate single crystals," *Physical Review Letters*, vol. 109, Article ID 097603, 4 pages, 2012.

[109] D. L. Corker, A. M. Glazer, R. W. Whatmore, A. Stallard, and F. Fauth, "A neutron diffraction investigation into the rhombohedral phases of the perovskite series PbZr1-xTixO_3," *Journal of Physics Condensed Matter*, vol. 10, no. 28, pp. 6251–6269, 1998.

[110] S. Adams, "Relationship between bond valence and bond softness of alkali halides and chalcogenides," *Acta Crystallographica B*, vol. 57, no. 3, pp. 278–287, 2001.

[111] I. D. Brown, "Recent developments in the methods and applications of the bond valence model," *Chemical Reviews*, vol. 109, no. 12, pp. 6858–6919, 2009.

[112] R. G. Burkovsky, A. V. Filimonov, A. I. Rudskoy, K. Hirota, M. Matsuura, and S. B. Vakhrushev, "Diffuse scattering anisotropy and inhomogeneous lattice deformations in the lead magnoniobate relaxor PMN above the Burns temperature," *Physical Review B*, vol. 85, no. 9, Article ID 094108, 2012.

[113] S. Vakhrushev, A. Nabereznov, S. K. Sinha, Y. P. Feng, and T. Egami, "Synchrotron X-ray scattering study of lead magnoniobate relaxor ferroelectric crystals," *Journal of Physics and Chemistry of Solids*, vol. 57, no. 10, pp. 1517–1523, 1996.

[114] H. Hiraka, S.-H. Lee, P. M. Gehring, G. Xu, and G. Shirane, "Cold neutron study on the diffuse scattering and phonon excitations in the relaxor $Pb(Mg_{1/3}Nb_{2/3})O_3$," *Physical Review B*, vol. 70, no. 18, Article ID 184105, pp. 1–7, 2004.

[115] S. Teslic, T. Egami, and D. Viehland, "Local atomic structure of PZT and PLZT studied by pulsed neutron scattering," *Journal of Physics and Chemistry of Solids*, vol. 57, no. 10, pp. 1537–1543, 1996.

[116] M. El Marssi, R. Farhi, J.-L. Dellis, M. D. Glinchuk, L. Seguin, and D. Viehland, "Ferroelectric and glassy states in La-modified lead zirconate titanate ceramics: a general picture," *Journal of Applied Physics*, vol. 83, no. 10, pp. 5371–5380, 1998.

[117] R. L. Withers, Y. Liu, and T. R. Welberry, "Structured diffuse scattering and the fundamental 1-d dipolar unit in PLZT (Pb1-yLay)1-α(Zr1-xTix)1-βO_3 (7.5/65/35 and 7.0/60/40) transparent ferroelectric ceramics," *Journal of Solid State Chemistry*, vol. 182, no. 2, pp. 348–355, 2009.

[118] Y. Terado, S. J. Kim, C. Moriyoshi, Y. Kuroiwa, M. Iwata, and M. Takata, "Disorder of Pb atom in cubic structure of $Pb(Zn_{1/3}Nb_{2/3})O_3$-$PbTiO_3$ system," *Japanese Journal of Applied Physics A*, vol. 45, no. 9B, pp. 7552–7555, 2006.

[119] J. Kuwata and K. Uchino, "Dielectric and piezoelectric properties of $0.91Pb(Zn_{1/3}Nb_{2/3})O_3$-$0.09PbTiO_3$ single crystals," *Japanese Journal of Applied Physics*, vol. 21, Article ID 1298, 1982.

[120] J. Kuwata, K. Uchino, and S. Nomura, "Phase transitions in the Pb $(Zn_{1/3}Nb_{2/3})O_3$-$PbTiO_3$ system," *Ferroelectrics*, vol. 37, pp. 579–582, 1981.

[121] J. S. Forrester, E. H. Kisi, K. S. Knight, and C. J. Howard, "Rhombohedral to cubic phase transition in the relaxor ferroelectric PZN," *Journal of Physics Condensed Matter*, vol. 18, no. 19, pp. L233–L240, 2006.

[122] E. H. Kisi and J. S. Forrester, "Crystal structure of the relaxor ferroelectric PZN: demise of the 'X-phase'," *Journal of Physics Condensed Matter*, vol. 17, no. 36, pp. L381–L384, 2005.

[123] P. Bonneau, P. Garnier, E. Husson, and A. Morell, "Structural study of PMN ceramics by X-ray diffraction between 297 and 1023 K," *Materials Research Bulletin*, vol. 24, no. 2, pp. 201–206, 1989.

[124] C. Stock, R. J. Birgeneau, S. Wakimoto et al., "Universal static and dynamic properties of the structural transition in $Pb(Zn_{1/3}Nb_{2/3})O_3$," *Physical Review B*, vol. 69, no. 9, Article ID 094104, 2004.

[125] H. You, "Diffuse X-ray scattering study of lead magnesium niobate single crystals," *Physical Review Letters*, vol. 79, no. 20, pp. 3950–3953, 1997.

[126] K. Hirota, Z.-G. Ye, S. Wakimoto, P. M. Gehring, and G. Shirane, "Neutron diffuse scattering from polar nanoregions in the relaxor $Pb(Mg_{1/3}Nb_{2/3})O_3$," *Physical Review B*, vol. 65, no. 10, Article ID 104105, 7 pages, 2002.

[127] G. Burns and F. H. Dacol, "Crystalline ferroelectrics with glassy polarization behavior," *Physical Review B*, vol. 28, no. 5, pp. 2527–2530, 1983.

[128] D. La-Orauttapong, J. Toulouse, J. L. Robertson, and Z.-G. Ye, "Diffuse neutron scattering study of a disordered complex perovskite $Pb(Zn_{1/3}Nb_{2/3})O_3$ crystal," *Physical Review B*, vol. 64, Article ID 212101, 4 pages, 2001.

[129] D. La-Orauttapong, J. Toulouse, Z.-G. Ye, W. Chen, R. Erwin, and J. L. Robertson, "Neutron scattering study of the relaxor ferroelectric (1-x)$Pb(Zn_{1/3}Nb_{2/3})O_{3-x}PbTiO_3$," *Physical Review B*, vol. 67, Article ID 134110, 10 pages, 2003.

[130] M. Soda, M. Matsuura, Y. Wakabayashi, and K. Hirota, "Superparamagnetism induced by polar nanoregions in relaxor Ferroelectric (1-x)$BiFeO_3$-$x BaTiO_3$," *Journal of the Physical Society of Japan*, vol. 80, no. 4, Article ID 043705, 2011.

[131] Y. Yoneda, K. Yoshii, S. Kohara, S. Kitagawa, and S. Mori, "Local structure of $BiFeO_3$-$BaTiO_3$ mixture," *Japanese Journal of Applied Physics*, vol. 47, no. 9, pp. 7590–7594, 2008.

[132] N. E. Brese and M. O'Keeffe, "Bond-valence parameters for solids. Bond-valence parameters for solids," *Acta Crystallographica B*, vol. 47, pp. 192–197, 1991.

[133] S. V. Krivovichev, "Derivation of bond-valence parameters for some cation-oxygen pairs on the basis of empirical relationships between r_o and b," *Zeitschrift für Kristallographie*, vol. 227, pp. 575–579, 2012.

[134] T. R. Welberry and D. J. Goossens, "Different models for the polar nanodomain structure of PZN and other relaxor

ferroelectrics," *Journal of Applied Crystallography*, vol. 41, no. 3, pp. 606–614, 2008.

[135] L. Xie, Y. L. Li, R. Yu et al., "Static and dynamic polar nanoregions in relaxor ferroelectric $Ba(Ti_{1-x}Sn_x)O_3$ system at high temperature," *Physical Review B*, vol. 85, Article ID 014118, 5 pages, 2012.

[136] Z. Guo, R. Tai, H. Xu et al., "X-ray probe of the polar nanoregions in the relaxor ferroelectric $0.72Pb(Mg_{1/3}Nb_{2/3})O_3$-$0.28PbTiO_3$," *Applied Physics Letters*, vol. 91, no. 8, Article ID 081904, 2007.

[137] S. B. Vakchrushev, B. E. Kvyatkovsky, A. A. Nabereznov, N. M. Okuneva, and B. P. Toperverg, "Neutron scattering from disordered perovskite-like crystals and glassy phenomena," *Physica B*, vol. 156-157, no. C, pp. 90–92, 1989.

[138] N. De Mathan, E. Husson, G. Calvarn, J. R. Gavarri, A. W. Hewat, and A. Morell, "A structural model for the relaxor $PbMg_{1/3}Nb_{2/3}O_3$ at 5 K," *Journal of Physics*, vol. 3, no. 42, article 011, pp. 8159–8171, 1991.

[139] G. Xu, G. Shirane, J. R. D. Copley, and P. M. Gehring, "Neutron elastic diffuse scattering study of $Pb(Mg_{1/3}Nb_{2/3})O_3$," *Physical Review B*, vol. 69, no. 6, Article ID 064112, 2004.

[140] J. Hlinka, J. Petzelt, S. Kamba, D. Noujni, and T. Ostapchuk, "Infrared dielectric response of relaxor ferroelectrics," *Phase Transitions*, vol. 79, no. 1-2, pp. 41–78, 2006.

[141] A. Al-Zein, B. Hehlen, J. Rouquette, and J. Hlinka, "Polarized hyper-Raman scattering study of the silent F_{2u} mode in $PbMg_{1/3}Nb_{2/3}O_3$," *Physical Review B*, vol. 78, no. 13, Article ID 134113, 7 pages, 2008.

[142] W. Dmowski, S. B. Vakhrushev, I.-K. Jeong, M. P. Hehlen, F. Trouw, and T. Egami, "Local lattice dynamics and the origin of the relaxor ferroelectric behavior," *Physical Review Letters*, vol. 100, no. 13, Article ID 137602, 2008.

[143] P. M. Gehring, H. Hiraka, C. Stock et al., "Polarized hyper-Raman scattering study of the silent F_{2u} mode in $PbMg_{1/3}Nb_{2/3}O_3$," *Physical Review B*, vol. 79, no. 22, Article ID 224109, 7 pages, 2009.

[144] A. Al-Zein, J. Hlinka, and J. Rouquette, "Soft mode doublet in $PbMg_{1/3}Nb_{2/3}O_3$ relaxor investigated with hyper-raman scattering," *Physical Review Letters*, vol. 105, no. 1, Article ID 017601, 2010.

[145] S. Tinte, B. P. Burton, E. Cockayne, and U. V. Waghmare, "Origin of the relaxor state in $Pb(B_xB'_{1-x})O_3$ perovskites," *Physical Review Letters*, vol. 97, no. 13, Article ID 137601, 2006.

[146] I. Grinberg, P. Juhás, P. K. Davies, and A. M. Rappe, "Relationship between local structure and relaxor behavior in perovskite oxides," *Physical Review Letters*, vol. 99, no. 26, Article ID 267603, 4 pages, 2007.

[147] A. Bosak, D. Chernyshov, S. Vakhrushev, and M. Krisch, "Diffuse scattering in relaxor ferroelectrics: true three-dimensional mapping, experimental artefacts and modelling," *Acta Crystallographica A*, vol. 68, no. 1, pp. 117–123, 2012.

[148] A. Bosak and D. Chernyshov, "On model-free reconstruction of lattice dynamics from thermal diffuse scattering," *Acta Crystallographica A*, vol. 64, no. 5, pp. 598–600, 2008.

[149] M. Paściak and T. R. Welberry, "Diffuse scattering and local structure modeling in ferroelectrics," *Zeitschrift Für Kristallographie*, vol. 226, pp. 113–1125, 2011.

[150] M. Sepliarsky and R. E. Cohen, "First-principles based atomistic modeling of phase stability in PMN-*x*PT," *Journal of Physics: Condensed Matter*, vol. 23, no. 43, Article ID 435902.

[151] I.-K. Jeong, T. W. Darling, J. K. Lee et al., "Direct observation of the formation of polar nanoregions in $Pb(Mg_{1/3}Nb_{2/3})O_3$ using neutron pair distribution function analysis," *Physical Review Letters*, vol. 94, no. 14, Article ID 147602, 2005.

[152] M. Paściak, T. R. Welberry, J. Kulda, M. Kempa, and J. Hlinka, "Polar nanoregions and diffuse scattering in the relaxor ferroelectric $PbMg_{1/3}Nb_{2/3}O_3$," *Physical Review B*, vol. 85, Article ID 224109, 2012.

[153] Q. M. Zhang, H. You, M. L. Mulvihill, and S. J. Jang, "An X-ray diffraction study of superlattice ordering in lead magnesium niobate," *Solid State Communications*, vol. 97, no. 8, pp. 693–698, 1996.

[154] T. Egami, H. D. Rosenfeld, B. H. Toby, and A. Bhalla, "Diffraction studies of local atomic structure in ferroelectric and superconducting oxides," *Ferroelectrics*, vol. 120, no. 1, pp. 11–21, 1991.

[155] H. D. Rosenfeld and T. Egami, "Model of local atomic structure in the relaxor ferroelectric $Pb(Mg_{1/3}Nb_{2/3})O_3$," *Ferroelectrics*, vol. 150, no. 1-2, pp. 183–197, 1993.

[156] J. Wen, G. Xu, C. Stock, and P. M. Gehring, "Response of polar nanoregions in 68%Pb $(Mg_{1/3}Nb_{2/3})O_3$-32%$PbTiO_3$ to a [001] electric field," *Applied Physics Letters*, vol. 93, no. 8, Article ID 082901, 2008.

[157] R. Blinc, V. Laguta, and B. Zalar, "Field cooled and zero field cooled ^{207}Pb NMR and the local structure of relaxor $PbMg_{1/3}Nb_{2/3}O_3$," *Physical Review Letters*, vol. 91, no. 24, Article ID 247601, 4 pages, 2003.

[158] Z.-G. Ye, Y. Bing, J. Gao et al., "Development of ferroelectric order in relaxor $(1\text{-}x)Pb(Mg_{1/3}Nb_{2/3})O_3$-$xPbTiO_3$ ($0 <\sim x \sim 0.15$)," *Physical Review B*, vol. 67, Article ID 104104, 8 pages, 2003.

[159] B. Mihailova, N. Waeselmann, B. J. Maier et al., "Chemically induced renormalization phenomena in Pb-based relaxor ferroelectrics under high pressure," *Journal of Physics*, vol. 25, no. 11, Article ID 115403, 2013.

[160] B. J. Maier, N. Waeselmann, B. Mihailova et al., "Structural state of relaxor ferroelectrics $PbSc_{0.5}Ta_{0.5}O_3$ and $PbSc_{0.5}Nb_{0.5}O_3$ at high pressures up to 30 GPa," *Physical Review B*, vol. 84, no. 17, Article ID 174104, 2011.

[161] A.-M. Welsch, B. J. Maier, J. M. Engel et al., "Effect of Ba incorporation on pressure-induced structural changes in the relaxor ferroelectric $PbSc_{0.5}Ta_{0.5}O_3$," *Physical Review B*, vol. 80, no. 10, Article ID 104118, 2009.

[162] B. Mihailova, R. J. Angel, A.-M. Welsch et al., "Pressure-induced phase transition in $PbSc_{0.5}Ta_{0.5}O_3$ as a model Pb-based perovksite-type relaxor ferroelectric," *Physical Review Letters*, vol. 101, Article ID 017602, 4 pages, 2008.

[163] N. Takesue, Y. Fujii, M. Ichihara, H. Chen, S. Tatemori, and J. Hatano, "Effects of B-site ordering/disordering in lead scandium niobate," *Journal of Physics Condensed Matter*, vol. 11, no. 42, pp. 8301–8312, 1999.

[164] N. Takesue, Y. Fujii, M. Ichihara, and H. Chen, "X-ray diffuse scattering study of glass-like transition behavior of relaxor lead scandium niobate," *Physics Letters A*, vol. 257, no. 3-4, pp. 195–200, 1999.

[165] C. Perrin, N. Menguy, E. Suard, C. Muller, C. Caranoni, and A. Stepanov, "Neutron diffraction study of the relaxor-ferroelectric phase transition in disordered $Pb(Sc_{1/2}Nb_{1/2})O_3$," *Journal of Physics Condensed Matter*, vol. 12, no. 33, pp. 7523–7539, 2000.

[166] G. A. Smolensky, *Ferroelectrics and Related Materials*, Academic Press, New York, NY, USA, 1981.

[167] S. N. Gvasaliya, B. Roessli, D. Sheptyakov, S. G. Lushnikov, and T. A. Shaplygina, "Neutron scattering study of $PbMg_{1/3}Ta_{2/3}O_3$ and $BaMg_{1/3}Ta_{2/3}O_3$ complex perovskites," *European Physical Journal B*, vol. 40, no. 3, pp. 235–241, 2004.

[168] R. D. Shannon, "Crystal physics, diffraction, theoretical and general crystallography," *Acta Crystallographica A*, vol. 32, no. 751, 1976.